AxCALacZ   AxCArGIFM

Fig. 2. Representative brain sections of rats treated with AxCALacZ as control (A) and AxCAGIFM (B). In rats treated with AxCALacZ, the tissue with stab wound tends to be concave from the surface of the brain. On the other hand, the rats treated with AxCArGIFM showed clear improvement around the stab wound compared with rats treated with AxCALacZ. The sections were stained with hematoxylin and eosin (H&E) staining at 17 days postoperation. Scale bar, 100 μm.

To maintain the GIF effect, we produced AxCArGIFM and administered it in the stab wound model. The administration of AxCArGIFM at an appropriate amount produced the desired results for the repair of the brain following stab wounds compared with AxCALacZ. In AxCArGIFM-administered rats, the levels of MAP-2 and GAP-43 were significantly higher than those in the control, whereas the level of GFAP was almost the same between the two groups.

GAP-43 is generally considered to be a marker of neurite outgrowth [1,16]. Although this finding seems to be in contrast with the function of GIF for neonatal neurons in vitro, which is considered to have an inhibitory effect on neurite outgrowth, GIF has also neuroprotective effects such as anti-oxidation. Therefore GIF may increase or sustain the content of GAP-43 compared with controls. Alternatively, GIF may affect the progression of neuronal stem/progenitor cells. Further studies are needed to

clarify the functional mechanism of GIF in detail by immunohistochemical methods using laser confocal scanning microscopy, extending the work we have already performed [10], and molecular genetic techniques. However, the finding in this paper will be a turning point for further studies.

Carrasco et al. stated that GIF-deficient mice with focal cryolesions did not differ from control mice [2]. On the other hand, we have demonstrated that AxCArGIFM could prevent degeneration of facial motoneurons following avulsion of the facial nerve [17]. Furthermore, in this study we have demonstrated that GIF can promote brain repair following brain injury due to stab wounds. GIF interestingly confers protective roles against not only oxidative stress [21,24] but also hypoxia [18]. MTs including GIF are promising as therapeutic agents not only for tissue repair following acute brain injury [4,13], but also for
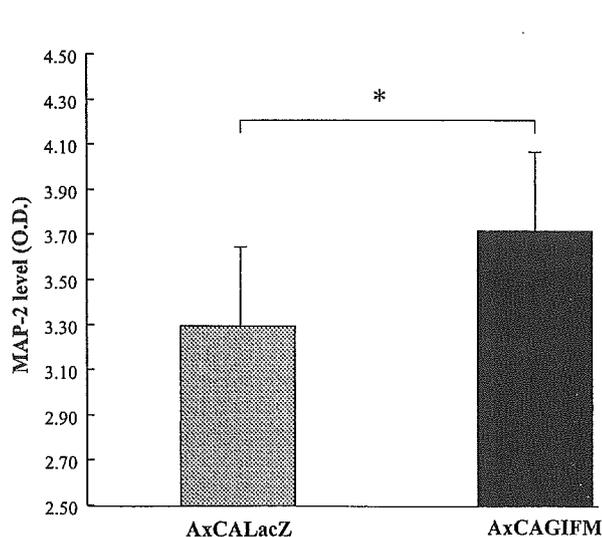

Fig. 3. MAP-2 level determined by immunoblotting. The MAP-2 level in AxCArGIFM-administered rats was significantly higher than that in AxCALacZ-administered rats ($n = 11$). $^*P < 0.05$.
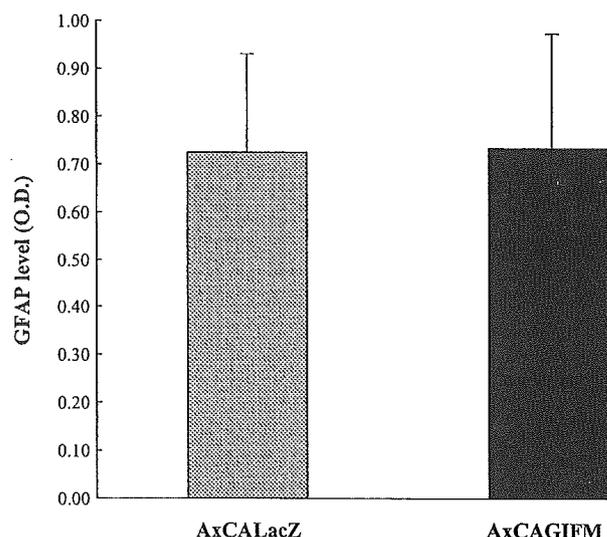

Fig. 4. GFAP level determined by immunoblotting. No significant difference could not be recognized between AxCArGIFM-administered rats and AxCALacZ-administered rats ($n = 11$).
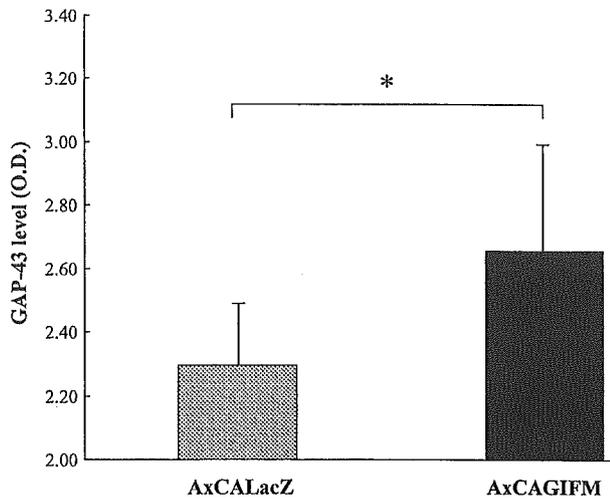
Fig. 5. GAP-43 level determined by immunoblotting. The GAP-43 level in AxCArGIFM-administered rats was significantly higher than that in AxCALacZ-administered rats $(n = 11)$. $^*P < 0.05$.

certain neurodegenerative diseases [6] because they have multi-functional potential including anti-oxidation and may have some effect on neurogenesis.

The experimental protocols were approved by the Animal Care and Use Committees of both the Tokyo Metropolitan Institute of Gerontology and the Tokyo Metropolitan Institute for Neuroscience.

Acknowledgements

References

[1] L.I. Benowitz, A. Rottenber, GAP-43: an intrinsic determinant of neuronal development and plasticity, Trends Neurosci. 20 (1997) 84–91.

[2] J. Carrasco, M. Penkowa, M. Giralt, J. Camats, A. Molinero, I.L. Campbell, R.D. Palmiter, J. Hidalgo, Role of metallothionein-III following central nervous system damage, Neurobiol. Dis. 13 (2003) 22–36.

[3] J.C. Erickson, G. Hollopeter, S.A. Thomas, G.J. Froelick, R.D. Palmiter, Disruption of the metallothionein-III gene in mice: analysis of brain zinc, behavior, and neuron vulnerability to metals, aging, and seizures, J. Neurosci. 17 (1997) 1271–1281.

[4] M. Giralt, M. Penkowa, N. Lago, A. Molinero, J. Hidalgo, Metallothionein-1 +2 protect the CNS after a focal brain injury, Exp. Neurol. 173 (2002) 114–128.

[5] M. Hiraiwa, J. Liu, A.-G. Lu, C.-I. Wang, R. Misasi, T. Yamauch, I. Hozumi, T. Inuzuka, J.S. O'Brien, Regulation of gene expression in response to brain injury: enhanced expression and altered splicing of rat prosaposin (SGP-1) mRNA in injured brain, J. Neurotrauma 20 (2003) 755–765.

[6] I. Hozumi, M. Asanuma, M. Yamada, Y. Uchida, Metallothionein and neurodegenerative diseases, J. Health Sci. 50 (2004) 323–331.

[7] I. Hozumi, F.-C. Chiu, W.T. Norton, Biochemical and immunohistochemical changes in glial fibrillary acidic protein after stab wounds, Brain Res. 524 (1990) 64–71.

[8] I. Hozumi, M. Hiraiwa, T. Inuzuka, Y. Yoneoka, K. Akiyama, R. Tanaka, K. Kikugawa, R. Nakano, S. Tsuji, J.S. O'Brien, Administration of prosaposin ameliorates spatial learning disturbance and reduces cavity formation following stab wounds in rat brain, Neurosci. Lett. 267 (1999) 73–76.

[9] I. Hozumi, T. Inuzuka, M. Hiraiwa, Y. Uchida, T. Anezaki, H. Ishiguro, H. Kobayashi, Y. Uda, T. Miyatake, S. Tsuji, Changes of growth inhibitory factor after stab wounds in rat brain, Brain Res. 688 (1995) 143–148.

[10] I. Hozumi, T. Inuzuka, H. Ishiguro, M. Hiraiwa, Y. Uchida, S. Tsuji, Immunoreactivity of growth inhibitory factor in normal rat brain and after stab wounds—an immunocytochemical study using confocal laser scan microscope, Brain Res. 741 (1996) 197–204.

[11] A.T. Miles, G.M. Hawksworth, J.H. Beattie, V. Rodilla, Induction, regulation, degradation, and biological significance of mammalian metallothioneins, Crit. Rev. Biochem. Mol. Biol. 35 (2000) 35–70.

[12] R.D. Palmiter, S.D. Findley, T.E. Whitemore, D.M. Durnam, MT-III, a brain-specific member of the metallothionein gene family, Proc. Natl. Acad. Sci. U.S.A. 89 (1992) 6333–6337.

[13] M. Penkowa, J. Hidalgo, Treatment with metallothionein prevents demyelination and axonal damage and increases oligodendrocyte precursors and tissue repair during experimental autoimmune encephalomyelitis, J. Neurosci. Res. 72 (2003) 574–586.

[14] C.J. Quaife, S.D. Findley, J.C. Erickson, G.J. Froelick, E.J. Kelly, B.P. Zambrowics, R.D. Palmiter, Induction of a new metallothionein isoform (MT-IV) occurs during differentiation of stratified squamous epithelia, Biochemistry 33 (1994) 7250–7259.

[15] C.J. Quaife, E.J. Kelly, B.A. Masters, R.L. Brister, R.D. Palmiter, Ectopic expression of metallothionein-III causes pancreatic acinar cell necrosis in transgenic mice, Toxicol. Appl. Pharmacol. 148 (1998) 148–157.

[16] A. Routtenberg, Protein kinase C activation leading to protein F1 phosphorylation may regulate synaptic plasticity by presynaptic growth, Behav. Neural Biol. 44 (1985) 186–200.

[17] T. Sakamoto, Y. Kawazoe, Y. Uchida, I. Hozumi, T. Inuzuka, K. Watabe, Growth inhibitory factor prevents degeneration of injured adult rat motoneurons, Neuroreport 14 (2003) 2147–2151.

[18] K. Tanji, Y. Irie, Y. Uchida, F. Mori, K. Satoh, Y. Mizushima, K. Wakabayashi, Expression of metallothionein-III induced by hypoxia attenuates hypoxia-induced cell death in vitro, Brain Res. 976 (2003) 125–129.

[19] S. Tsuji, H. Kobayashi, Y. Uchida, Y. Ihara, T. Miyatake, Molecu cloning of human growth inhibitory factor cDNA and its down-regulation in Alzheimer's disease, EMBO J. 11 (1992) 4843–4850.

[20] Y. Uchida, Regulation of growth inhibitory factor expression by epidermal growth factor and interleukin-1β in cultured rat astrocytes, J. Neurochem. 73 (1999) 1945–1953.

[21] Y. Uchida, F. Gomi, T. Masumizu, Y. Miura, Growth inhibitory factor prevents neurite extension and the death of cortical neurons caused by high oxygen exposure through hydroxyl radical scavenging, J. Biol. Chem. 277 (2002) 32353–32359.

[22] Y. Uchida, K. Takio, K. Titani, Y. Ihara, M. Tomonaga, The growth inhibitory factor that is deficient in the Alzheimer's disease brain is a 68 amino acid metallothionein-like protein, Neuron 7 (1991) 337–347.

[23] B.L. Vallee, The function of metallothionein, Neurochem. Int. 27 (1995) 23–33.

[24] H.J. You, K.J. Lee, H.G. Jeong, Overexpression of human metallothionein-III prevents hydrogen peroxide-induced oxidative stress in human fibroblasts, FEBS Lett. 521 (2002) 175–179.

ORIGINAL ARTICLE

Adenoviral GDNF gene transfer enhances neurofunctional recovery after recurrent laryngeal nerve injury

K Araki[1], A Shiotani[1], K Watabe[2], K Saito[1], K Moro[1] and K Ogawa[1]

[1]Department of Otolaryngology, Head and Neck Surgery, Keio University School of Medicine, Shinjukuku, Tokyo, Japan and [2]Department of Molecular Neuropathology, Tokyo Metropolitan Institute for Neuroscience, Fuchu, Tokyo, Japan

To assess the possibility of gene therapy for recurrent laryngeal nerve (RLN) injury, we examined functional and histological recovery after glial cell line-derived neurotrophic factor (GDNF) gene transfer in a rat RLN crush model. Adenoviral vector encoding β-galactosidase gene (AxCA-LacZ) or human GDNF gene (AxCAhGDNF) was injected into the crush site of the RLN. Neurons in the nucleus ambiguus on the crushed side were labeled with X-gal or GDNF immmunohistochemistry after AxCALacZ or AxCAhGDNF injection. Reverse transcription-polymerase chain reaction analysis revealed expression of human GDNF mRNA transcripts in brainstem tissue containing the nucleus ambiguus on the crushed side after AxCAhGDNF injection. Animals injected with AxCAhGDNF displayed significantly improved motor nerve conduction velocity of the RLN and recovery rate of vocal fold movement at 2 and 4 weeks after treatment as compared to controls. AxCAhGDNF-injected animals showed a significantly larger axonal diameter and improved remyelination in crushed RLN as compared to controls. Adenoviral GDNF gene transfer may thus promote laryngeal function recovery after RLN injury. Inoculation of adenoviral vector containing the GDNF gene at the site of damage soon after nerve injury may assist patients with laryngeal paralysis caused by nerve injury during head and neck surgery.
Gene Therapy (2006) 13, 296–303. doi:10.1038/sj.gt.3302665; published online 27 October 2005

Introduction

The recurrent laryngeal nerve (RLN) comprises neurites of motor, sensory and autonomic neurons. One of the most significant laryngeal impairments caused by RLN injury is incomplete glottic closure, which induces dysphonia, dysphagia and aspiration pneumonia. These symptoms are associated with decreased quality of life. RLN injury can be caused by direct invasion of malignant tumor, such as thyroid or esophageal cancer, surgical ablation of the neck or mediastinum, thoracic aortic aneurism and intubation.

Medialization procedures (vocal fold injection, thyroplasty and arytenoid adduction) are commonly performed to manage unilateral vocal fold palsy, and can improve symptoms by enhancing glottic closure. However, these only achieve vocal fold medialization by static changes in vocal fold tissue or the laryngeal framework, and such deficits can never be neurologically restored.[1] Voice therapy is effective only for mild cases and reinnervation procedures have been attempted in very few cases.[2–4] Reinnervation procedures (neural anastomosis, nerve graft, etc.) for the RLN may improve voice quality through restoration or preservation of laryngeal muscle tone and have the potential to restore vocal fold mobility.[5,6] However, this procedure appears to have had little impact on the recovery of dynamic laryngeal function and is not widely accepted as a treatment option. The failure of reinnervation procedures is the result of multiple factors, including decreased motor fiber density, existing laryngeal muscle atrophy, central motoneuron loss in the nucleus ambiguus, and inappropriate or misdirected innervation by antagonistic motoneurons.[7,8]

The discovery of neurotrophic factors that support neuronal survival during development and neuronal function throughout adulthood has generated broad interest in the use of these factors in facilitating recovery after peripheral nerve injury. A multitude of neurotrophic factors have been shown to prevent motoneuron loss, enhance nerve sprouting, preserve motor endplate morphology, and promote reinnervation.[9–15] For example, glial cell line-derived neurotrophic factor (GDNF), brain-derived neurotrophic factor, neurotrophin (NT)-3, NT-4/5 and ciliary neurotrophic factor have been shown to prevent the loss of facial and spinal motoneurons after axotomy in neonatal rodents.[16–18] Of these, GDNF offers powerful survival-promoting effects on motor neurons *in vitro* and *in vivo*, and promotes nerve regeneration after injury.[19–22] Overexpression of GDNF produces hyperinnervation of neuromuscular junctions,[23] and expression of endogenous GDNF is increased early

following peripheral nerve injury.[24] The use of GDNF and other neurotrophic factors may prove beneficial for the treatment of peripheral nerve injuries.

Application of neurotrophic factors is hampered by a lack of efficient means of delivery to the peripheral nerves and brain. Direct injection of therapeutic peptides into CNS parenchyma may cause further injury to the CNS. When delivered through oral or systemic routes, these peptides are not feasible due to a short half-life *in vivo* and inability to cross the blood–brain barrier, and often cause harmful adverse effects.[14,15,25] Gene therapy is a strategy for transferring the DNA coding for neurotrophic factors into the CNS or peripheral nerve. This would provide a mechanism for single administration of a vector to achieve limited long term, steady levels of gene product using common routes of delivery.[26,27]

To overcome the problems concerning RLN reinnervation failure, we have demonstrated the potential of gene therapy. Insulin-like growth factor (IGF)-I gene transfer to denervated thyroarytenoid (TA) muscle has been shown to prevent muscle atrophy while improving motor endplate morphology in a rat laryngeal paralysis model,[28,29] and adenoviral vector-mediated GDNF gene transfer prevents motor neuron loss in the nucleus ambiguus in a rat vagal nerve avulsion model.[30] Although our previous studies have demonstrated histological improvements after therapeutic gene transfer, neurofunctional improvement has not previously been clarified. In the present study, to assess the possibility of gene therapy for the recovery of neurological function after RLN injury, we examined the electrophysiological and histological therapeutic effects of adenoviral GDNF gene transfer in an adult rat RLN crush model.
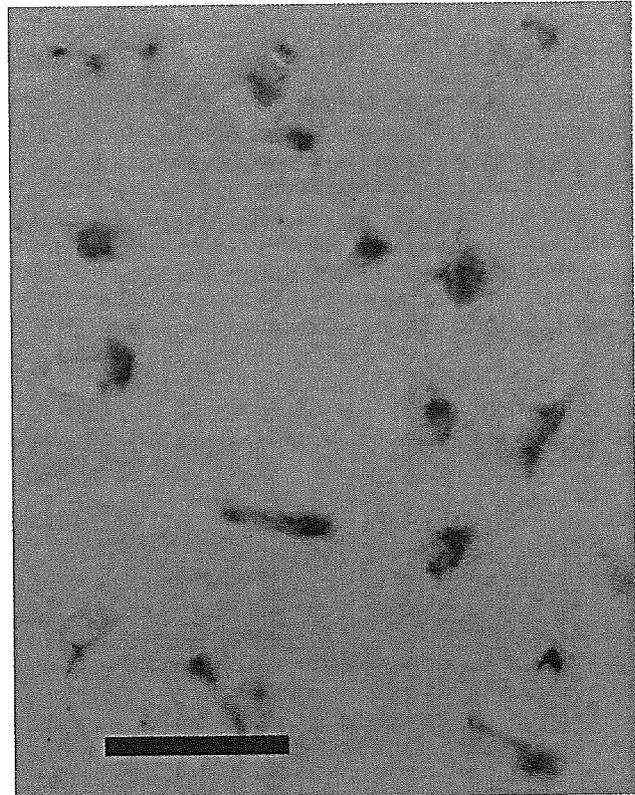

Figure 1   X-gal histochemical staining in the brainstem. At 4 days after RLN crush and intraneural injection of AxCALacZ into the RLN crush site, motor neurons in the nucleus ambiguus were clearly labeled with X-gal. No motoneurons or axons were labeled in the contralateral nucleus ambiguus. Scale bar, 50 μm.

Results

Gene expression in nucleus ambiguus

To investigate whether foreign gene transfer can be achieved by adenoviral vector in the RLN crush model, we first injected adenoviral vector encoding β-galactosidase gene (AxCALacZ) directly into the nerve after left RLN crush injury in adult rats. At 4 days after crush and injection of AxCALacZ, motoneurons of the nucleus ambiguus and associated axons were clearly labeled on X-gal histochemistry (Figure 1). No motoneurons or axons were labeled in the contralateral nucleus ambiguus. We subsequently injected human GDNF gene (AxCAhGDNF) into crushed animals and examined the expression of exogenous GDNF by reverse transcription-polymerase chain reaction (RT-PCR) and GDNF immnohistochemistry. At 4 days after left RLN crush and AxCAhGDNF injection, RT-PCR analysis revealed the expression of virus-induced human GDNF mRNA transcripts in brainstem tissue containing the nucleus ambiguus on the treated side (Figure 2). Virus-induced human GDNF mRNA was not detected on the contralateral side by RT-PCR. At 5 days after left RLN crush and AxCAhGDNF injection, GDNF immnohistochemistry showed expression of virus-induced human GDNF in motoneurons of the nucleus ambiguus on the treated side (Figure 3). No motoneurons or axons were labeled in the contralateral nucleus ambiguus. These results
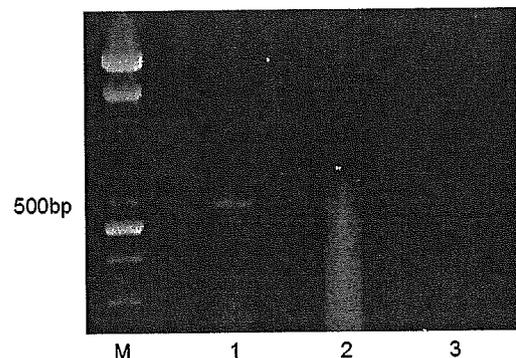

Figure 2   RT-PCR analysis of brainstem tissue including nucleus ambiguus 4 days after RLN crush and AxCAhGDNF treatment. Lane M, size markers; Lane 1, brainstem tissue on the treated side with reverse transcription; Lane 2, brainstem tissue on the treated side without reverse transcription; and Lane 3, brainstem tissue on the contralateral (nontreated) side with reverse transcription. Expression of virus-induced human GDNF mRNA transcripts in brainstem tissue on the treated side. No virus-induced human GDNF mRNA was detected on the contralateral side.

indicate that, after injection to injured axons, virus vectors were delivered to soma of motoneurons through retrograde axonal flow and the virus-encoded foreign gene was successfully induced.
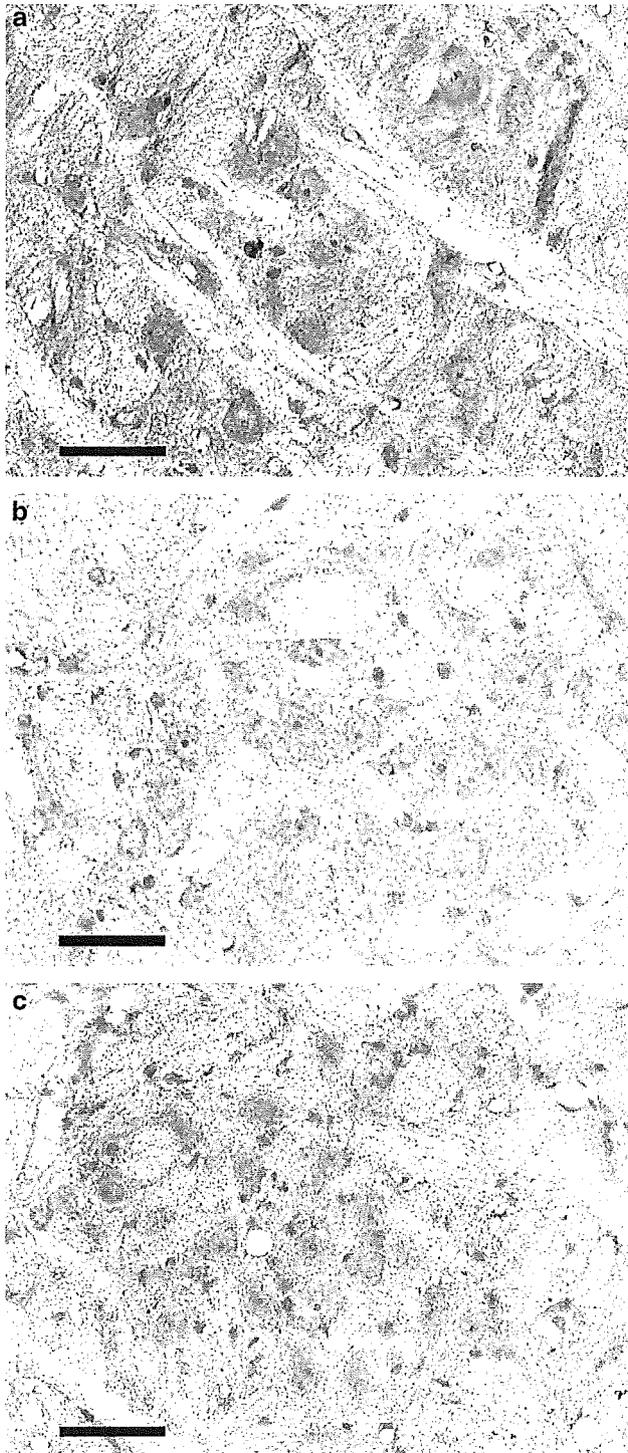
Figure 3 GDNF immunohistochemical staining in the brainstem. (a) The nucleus ambiguus on the treated side of AxCAhGDNF-injected animal. (b) The nucleus ambiguus on the contralateral (nontreated) side of AxCAhGDNF-injected animal. (c) The nucleus ambiguus of RLN crush (control) animal. At 5 days after RLN crush and intraneural injection of AxCAhGDNF into the RLN crush site, motor neurons in the nucleus ambiguus were clearly labeled with GDNF. No motoneurons were labeled in the nucleus ambiguus of contralateral side or RLN crush (control) animal. Scale bars, 50 μm.

Neurofunctional recovery after adenoviral GDNF gene transfer

We injected AxCAhGDNF (Group I), AxCALacZ (Group II), or nothing (Group III) after left RLN crush, and examined the effects of GDNF gene transfer on neurofunctional recovery. Representative electromyography (EMG) findings for Groups I, II and normal RLN are shown in Figure 4. EMG of AxCAhGDNF-injected rats showed shorter latency and shorter time lag of latency compared with AxCALacZ-injected rat, and the potential wave of AxCAhGDNF-injected rats was substantially similar to those in normal rats.

Mean ($\pm$s.d.) motor nerve conduction velocity (MNCV) in Group I was 31.49 ± 7.03 m/s at 2 weeks and 35.59 ± 6.28 m/s at 4 weeks. Normal MNCV of the RLN was 41.38 ± 7.23 m/s ($n = 4$). MNCV of AxCAhGDNF-injected animals thus recovered close to normal levels. MNCV in Group II was 12.59 ± 1.43 m/s at 2 weeks and 19.87 ± 3.05 m/s at 4 weeks, while MNCV in Group III was 17.34 ± 4.25 m/s at 2 weeks and 17.24 ± 3.18 m/s at 4 weeks. At both 2 and 4 weeks after RLN crush, MNCV was markedly reduced in Groups II and III. MNCV was thus significantly faster in Group I than in Groups II and III ($P < 0.05$) (Figure 5), indicating better neurofunctional recovery.

Recovery of vocal fold movement

The number of rats displaying obvious recovery of left vocal fold movement was 4/4 (100%) at 2 weeks and 4/4 (100%) at 4 weeks in Group I, 1/4 (25%) at 2 weeks and 1/4 (25%) at 4 weeks in Group II, and 0/4 (0%) at 2 weeks and 2/4 (50%) at 4 weeks in Group III. Recovery of vocal fold movement was thus significantly better in Group I than in Groups II and III ($P < 0.05$) (Table 1).

Morphometry results of RLN section

Diameters of axons were measured from left RLN sections. Representative cross-sections of RLN samples stained using epon/toluidine blue are shown in Figure 6. Mean diameters of axons and a histogram of axon diameters in normal rats, in Groups I and III are presented in Figure 7. Mean axon diameter was 6.28 ± 0.43 μm in normal rats, 4.76 ± 0.62 μm in Group I and 2.67 ± 0.10 μm in Group III. Mean axon diameter in group I was recovered to almost normal level, significantly larger than in Group III ($P < 0.05$). Histograms of axon diameter demonstrated that Group I displayed a reduction in the number of small axons and an increase in the number of larger axons compared with Group III.

Discussion

Injection of viral vector into nerves has been demonstrated in both spinal cord[31,32] and peripheral nerves.[33,34] The remote injection method of adeno-associated or adenoviral vectors into RLN is reportedly useful for delivering therapeutic gene products to the CNS.[35,36] Virus vector injected directly into the nerve is transported in a retrograde manner to the soma of neurons, and virus-induced foreign genes are thus induced in neurons. Our study showed that by direct injection to the RLN, AxCALacZ could transduce the β-galactosidase gene in the nucleus ambiguus as detected by X-gal histochemistry, and AxCAhGDNF could transduce the
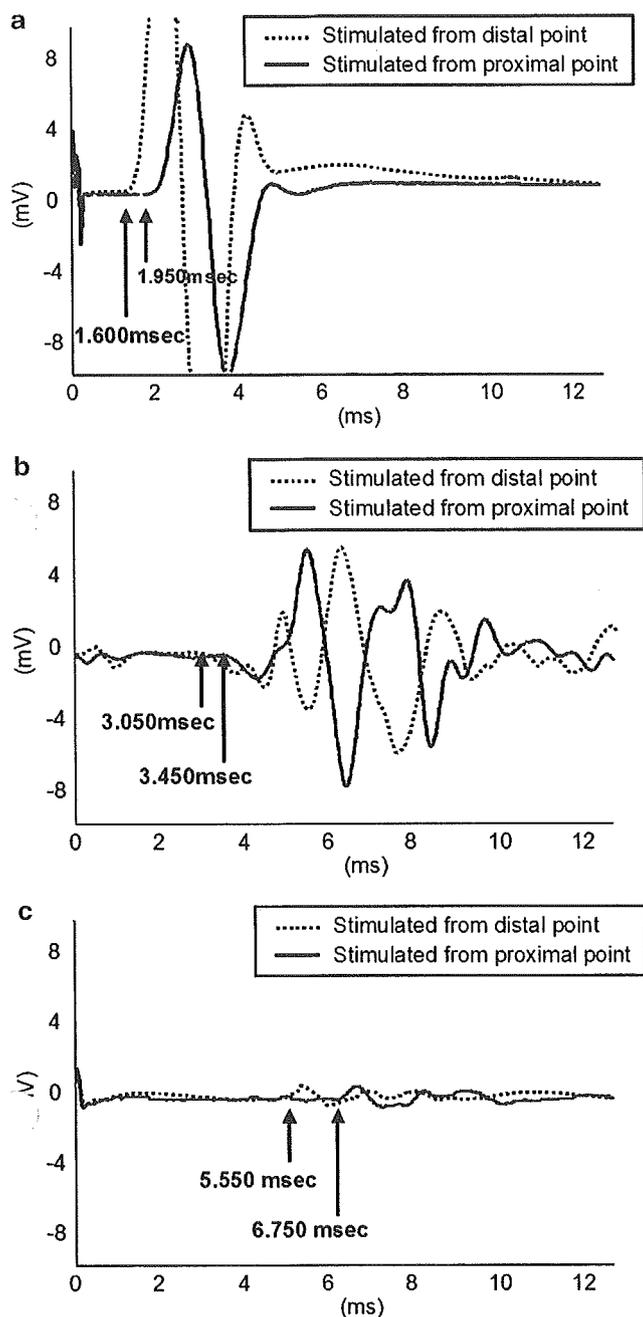
Figure 4 Electromyography of thyroarytenoid muscle. Representative evoked EMG obtained by left RLN stimulation. (a) Normal animals, (b) AxCAhGDNF-injected animals and (c) AxCALacZ-injected animals. EMG in AxCAhGDNF-injected rat revealed big action potential wave and shorter latency (b). Conversely, EMG in control rat showed small, unclear action potentials and delayed latency (c).

Figure 5 MNCV at 2 and 4 weeks after injury ($n = 4$). Significant differences are apparent between AxCAhGDNF- and AxCALacZ-injected animals, and between AxCAhGDNF-injected and RLN crush animals ($P < 0.05$) at 2 and 4 weeks after injury. MNCV in AxCAhGDNF-injected animals recovered favorably and was comparable to normal rat. GDNF gene expression offers strong protective and regenerative effects against motor nerve injury.

Table 1 Vocal fold movement recovery in each group

	2 weeks	4 weeks
AxCAhGDNF	4/4]*	4/4]*
AxCALacZ	1/4]	1/4]
Crush	0/4]	2/4]

Numerators show number of animals with vocal fold movement recovery. Denominators show number of animals observed. AxCAhGDNF-injected animals showed significantly better recovery rate for vocal fold movement compared to control animals (AxCALacZ-injected and RLN crush) at 2 and 4 weeks after injury, indicating strong functional recovery following GDNF gene transfer.
*$P < 0.05$.

hGDNF gene in the nucleus ambiguus as detected by RT-PCR and GDNF immnohistochemistry.

Remote injection of viral vectors does not appear to cause significant additional neuronal injury. Rubin et al.[36] demonstrated that no significant difference existed in percentage of nerve–endplate contacts between an RLN crushed-nerve group and a group with crush injury followed by virus injection. Our data support these findings. MNCV of the RLN did not differ signif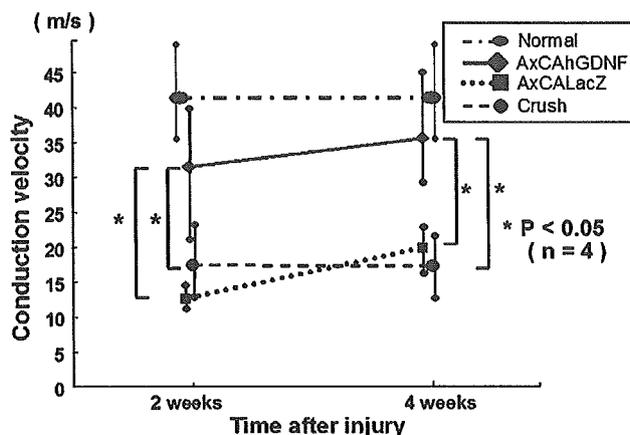icantly between the crushed-nerve group and the group with crush injury followed by AxCALacZ injection. Although the exact degree of nerve injury caused by the injection process itself is unclear, remote injection of adenoviral vector does not cause significant additional injury after crush and appears to represent a safe way to deliver viral vectors to the CNS.

Nerve crush is a reproducible injury that has been shown to yield a consistent degree of nerve injury.[37,38] This process induces Sunderland second-degree injury (axonotmesis), which involves injury to the axon such that Wallerian degeneration occurs distal to the injury, with only rare and minor features of first- and third-degree injury.[39] This model is ideal for exploring the effects of remotely injected viral vectors, providing an intact nerve for injection and retrograde axonal transport of virus. Recovery is associated with axonal sprouting with the intact individual endoneural tubes of Schwann cell basal lamina.[40]

Bridge et al.[38] demonstrated that in the various methods of delivering crush injury in rat sciatic nerve, the functional and histological responses to crush are identical. Their results also showed that MNCV recovered to almost normal levels and only minimal histolo-
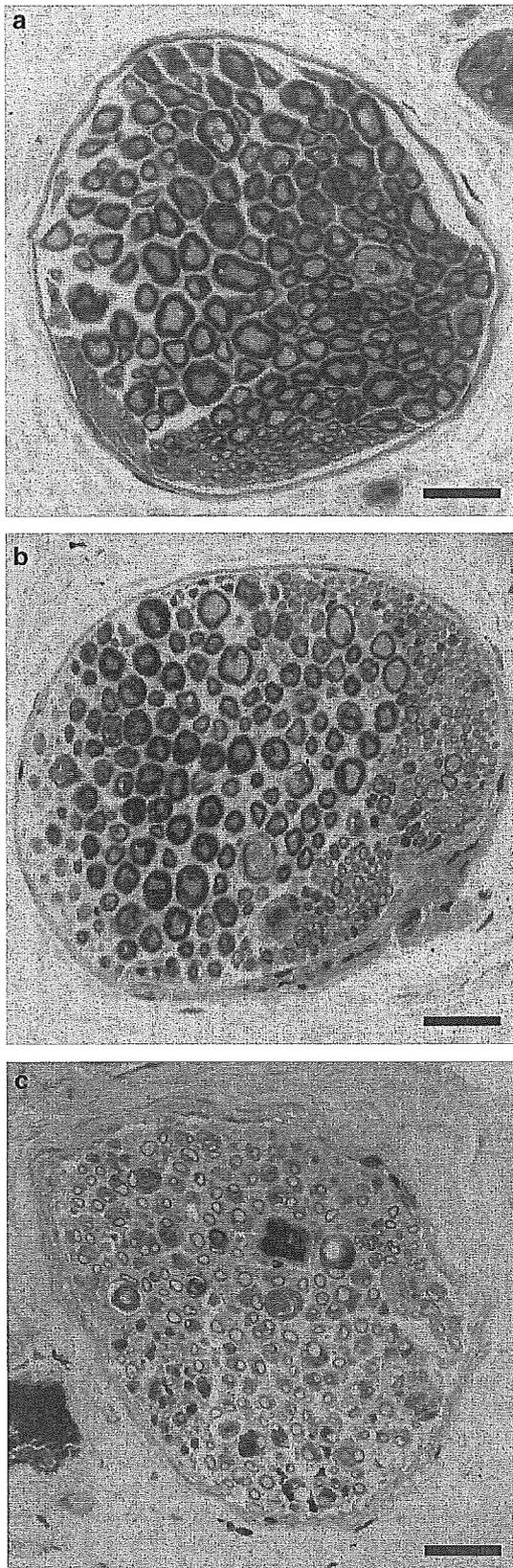
Figure 6 Photomicrographs of sectioned RLN stained with epon/ toluidine blue at 5 mm distal from crush site at 2 weeks after injury. (a) Normal, (b) AxCAhGDNF-injected animal and (c) RLN crush animal. Control animal with crush injury displays atrophied and demyelinated axons (c). However, in AxCAhGDNF-treated animal (b), better myelination and thick axons are observed, comparable to those in normal rat (a). Scale bars, 20 μm.
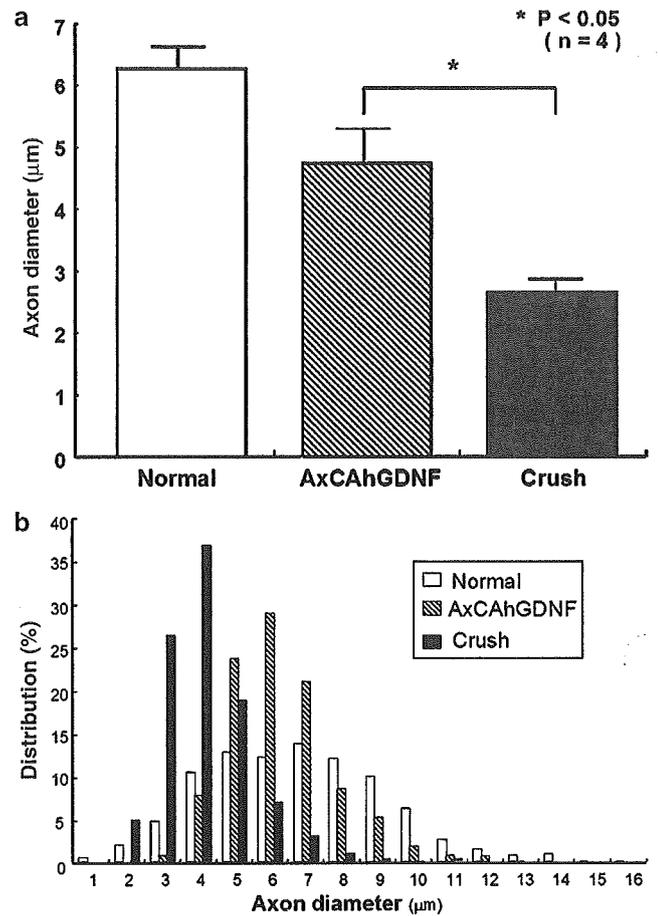

Figure 7 Axonal diameters 2 weeks after injury. (a) Mean axonal diameter for each nerve fiber ($n = 4$). Significant differences exist between AxCAhGDNF-injected animals and RLN crush animals ($P < 0.05$) at 2 weeks after injury, indicating better myelination and axon preservation in AxCAhGDNF-injected animals. (b) Distribution of axonal diameters. Histogram shows the total number of axonal diameters in AxCAhGDNF-injected and RLN crush animals ($n = 4$). Histogram of diameters reveals a reduced number of small axons and an increased number of larger axons in Group I compared with Group III.

gical abnormalities persisted with every crush method after 8 weeks and that electrophysiological recove paralleled functional recovery. The present study assessed neurofunctional recovery 2 or 4 weeks after surgery, demonstrating enhancement of motor nerve recovery based on neurofunctional and laryngeal functional data. The timing of assessment was appropriate for the regenerative process of peripheral nerves and our results demonstrate that early neurofunctional recovery might preserve good laryngeal function.

MNCV for the injured nerve is a commonly used physiological measure to evaluate peripheral nerve function in the rat nerve injury model.[37,38,41] In this study, the latency of compound muscle action potential from the TA muscle was recorded, and MNCV was calculated from the latencies of action potential and distance between the two stimulating points. Control animals injected with or without AxCALacZ displayed a markedly slowed MNCV that did not change between 2 and 4 weeks after injury. These results are consistent with limited regeneration of the nerve in control animals that did not improve even up to 4 weeks after injury.

After nerve injury, despite the occurrence of some degree of spontaneous functional recovery, complete functional recovery does not occur due to limited regenerative potential. The primary mechanical trauma causes disruption of the neuron and axon. Damage is due to ischemia at the injury site, shifts in electrolyte concentrations and excessive release of excitatory amino acids.[42] These processes initiate a cytotoxic-signaling cascade and myelin destruction, impeding axonal regrowth. In our study, animals injected with AxCAhGDNF exhibited significant improvements in MNCV compared to control animals, reaching almost normal levels by 2 and 4 weeks after treatment.

We also demonstrated that AxCAhGDNF-injected animals show significant improvements in recovery of vocal fold movement, axonal diameter and myelination, compared to control animals. Thickening of axon diameter and enhancement of myelination are considered to contribute to increases in MNCV. These regenerative effects on the nerve might finally achieve recovery of dynamic laryngeal function (recovery of vocal fold movement).

To minimize the deleterious effects of early trauma and promote and guide axonal regrowth, the delivery of neurotrophic factors has emerged as a promising strategy to manipulate for axonal regrowth in the early phase. This study demonstrated the enhancement of neurofunctional recovery after remote injection of adenovirus vector coding for the GDNF gene into crushed RLN over the course of a few weeks. The vocal folds are extremely delicate structures, and imperceptible injuries can result in excessive vocal complications. Extended injury results in atrophy of the laryngeal muscles, motoneuron loss in the nucleus ambiguus, and decreases in both motor axon density and nerve–endplate contact. Early recovery from axonal degeneration is important for preservation and recovery of laryngeal function. Again, the present methods achieved good preservation and facilitated recovery of laryngeal function.

Laryngeal paralysis most often occurs clinically as a result of vagal nerve or RLN injury after surgical ablation of a tumor involving the head and neck region. If the nerve is injured during surgery, direct injection of the vector into the nerve might prevent paralysis. Alternatively, when paralysis becomes apparent on extubation, the vector can be injected into the nerve after reintubation and opening the wound.

The adenovirus vector was used in this study. For clinical applications, controversy remains regarding the potential risks of virus-mediated gene therapy,[43–45] particularly when applied to nonlethal benign diseases such as laryngeal paralysis. To overcome this problem, safety of the vector must be demonstrated prior to clinical application. Preliminary experiments of nonviral gene transfer systems are also currently underway.

Our previous reports analyzed prevention of motoneuron death[30] and improvements in motor endplate morphology and muscle atrophy using histological methods.[28–30,46] The present study analyzed neurological function using electrophysiological examination in vivo and demonstrated neurofunctional recovery. This report carries a higher clinical impact than our previous reports. Adenoviral GDNF gene therapy may save patients with laryngeal paralysis caused by nerve injury during head and neck surgery, by inoculation of the vector at site of nerve damage immediately after injury. These results may open up clinical applications for GDNF gene therapy, not only for laryngeal paralysis, but also for all forms of peripheral motor nerve paralysis.

Materials and methods

Adenovirus preparation
Generation of replication-defective recombinant adenovirus carrying human GDNF cDNA (AxCAhGDNF) and bacterial β-galactosidase gene (AxCALacZ) has been described elsewhere.[46,47] Recombinant adenoviral vectors were propagated and isolated from 293 cells, and purified by two rounds of CsCl centrifugation. Bioactivities of AxCAhGDNF for fetal rat mesencephalic and spinal motoneuron cultures in vitro have previously been demonstrated.[46,48]

Animals and surgical procedures
A total of 32 adult male Sprague–Dawley rats (12-weeks old, 340–360 g) were used in these experiments. Animals were anesthetized using ketamine (100 mg/kg, intraperitoneal) and xylazine (10 mg/kg, intraperitoneal) and a midline vertical cervical incision was made through the skin. The submandibular glands and strap muscles were divided to expose trachea, thyroid and larynx. Under a dissecting microscope, the left RLN was exposed just inferior to the left lobe of the thyroid gland. At a point 10 mm proximal to the inferior border of the thyroid gland, the RLN was crushed once with a pair of forceps for exactly 60 s. Crush pressure of forceps was about 80 MPa and crush width was 2 mm. Direct laryngoscopy was performed to confirm left vocal fold paralysis. All procedures were performed in an identical manner by the same investigator using the same equipment.

Rats were randomly assigned to three groups (Groups I–III). In Group I ($n = 10$), about 3 μl of AxCAhGDNF (1×10^{10} PFU/ml) was injected at the crush point using a Nanoliter 2000 oocyte microinjector (World Precision Instruments, Sarasota, FL, USA) and micromanipulator immediately after nerve crush. In Group II ($n = 10$), AxCALacZ (1×10^{10} PFU/ml) was injected in an identical procedure. In Group III ($n = 8$), the RLN was crushed but no viral vector was injected. A glass micropipette was used for direct nerve injection and inserted beneath the perineurium with gentle countertraction of the nerve using microforceps. The strap muscles were repositioned, and the skin was sutured closed. Normal nerve conduction velocity in the RLN was measured using four rats without crush injury or vector injection.

Reverse transcription-polymerase chain reaction
At 4 days after left RLN crush and injection of AxCAhGDNF, animals were euthanized with a lethal dose of ketamine, and brainstem tissue around the nucleus ambiguus was selectively collected under microscopy. Total RNA was isolated from tissue using RNA isolation reagent (Trizol, Invitrogen, Carlsbad, CA, USA) in accordance with the instructions from the manufacturer, and treated with RNase-free DNase (Invitrogen, Carlsbad, CA, USA). First-strand cDNA was synthesized from 380 ng of total RNA using a random primer and Superscript II reverse transcriptase (Invitrogen, Carlsbad, CA, USA) for one PCR analysis.

PCR reactions were performed in PCR buffer containing cDNA template, 200 mM dNTPs, 2 mM $MgCl$, 20.2 mM of each primer and 25 U/ml of Taq DNA polymerase (TaKaRa, Osaka, Japan). Specific oligonucleotide primers for PCR were designed to amplify adenovirus-derived human GDNF cDNA (forward, 5'-ATGAAGTTATGGGA TGTCGT-3'; reverse, 5'-TCACCAGCCTTCTATTTCTG-3'), which produces 511-bp amplified product.[46] The PCR amplification program comprises 40 cycles of: denaturation at 95°C for 1 min, annealing at 55°C for 90 s and extension at 72°C for 90 s. For negative control reactions, nonreverse transcripted RNA samples and reverse-transcripted brain tissue of nontreated side were processed for PCR. PCR products were subjected to electrophoresis on a 2% agarose gel stained using ethidium bromide.

Histological analysis

For X-gal histochemistry, rats ($n = 2$ from Group II) at 4 days after left RLN crush and AxCALacZ injection were anesthetized using ketamine and xylazine, and transcardially perfused with 4% paraformaldehyde in PBS. Brainstem tissue was dissected, immersion-fixed in the same fixative for 2 h, cryoprotected in 30% sucrose in PBS, and serial transverse frozen sections were cut at 16 μm. Cryostat sections were incubated overnight at 37°C in a solution containing 5 mM potassium ferricyanide, 5 mM potassium ferrocyanide, 2 mM magnesium chloride, and 1 mg/ml of 5-bromo-4-chloro-3-indolyl-b-D galactopyranoside (X-gal; Invitrogen) in PBS. Sections were then rinsed and counterstained with eosin.

For GDNF immnohistochemistry, rats ($n = 2$ from Group I) at 5 days after left RLN crush and AxCAhGDNF injection were anesthetized and transcardially perfused with 4% paraformaldehyde in PB. Brainstem tissue was dissected, immersion-fixed in the same fixative for 2 h, cryoprotected in 30% sucrose in PBS, and serial transverse frozen sections were cut at 16 μm. Sections were pretreated with 0.3% H_2O_2 in PBS, rinsed in 0.1% Triton X-100 in PBS (T-PBS) and preincubated in 3% normal goat serum in T-PBS. After treatment using an ABC blocking kit (Vector, Burlingame, CA, USA) according to the manufacturer's instructions, sections were incubated overnight at 4°C with rabbit polyclonal antibody to GDNF (Santa Cruz Biotech, Santa Cruz, CA, USA) at a dilution of 1:1000, followed by incubation with biotinylated anti-rabbit IgG at a dilution of 1:100 and ABC reagent (Vector, Burlingame, CA, USA), visualized by 3,3'-diaminobenzidine tetrahydrochloride (DAB)-H_2O_2 solution and counterstained with hematoxylin.

For analysis of RLN section morphometry, left RLNs were excised 2 weeks after surgery and fixed in PBS containing 4% paraformaldehyde/2.5% glutaraldehyde at 4°C for 3 days. Sections were then postfixed in 1% osmium tetroxide, dehydrated through graded ethanol steps, and embedded in Epon 812 (Polysciences, Warrington, PA, USA). At 5 mm distal from the crush site, semithin sections of left RLN at 1 μm thickness were stained using toluidine blue. Digitized images of the entire axonal area were acquired using a CCD camera (PDMC II; Polaroid, Waltham, MA, USA) mounted on an E600 light microscope (Nikon, Tokyo, Japan) with a ×100 objective lens and the entire axonal area of each nerve sampled ($n = 4$) was evaluated using Micro Analyzer version 1.1 software (Nihon Poladigital, Tokyo, Japan) on the computer.

Neurofunctional analysis

To assess neurofunctional recovery, rats at 2 or 4 wee. after operation were subjected to measurement of MNCV. Animals were anesthetized and the left RLN was exposed and dissected inferior to the left lobe of the thyroid gland, as described above. The strap muscles were sectioned to expose the larynx, and a laryngeal fissure was made. The left TA muscle was stabbed through the fissure with a needle concentric electrode for recording. To stimulate the left RLN, two bipolar hook electrodes were placed and hooked into the left RLN. One was placed inferior to the left lobe of the thyroid as a distal stimulator, the other at 16 mm proximal to the distal electrode as a proximal stimulator. The nerve was maximally stimulated and compound muscle action potentials in TA muscle were recorded using a Power Lab computer-assisted electromyography machine (AD Instruments, Colorado Springs, CO, USA). Maximal stimulation was achieved by increasing current output until no further change in amplitude of the compound action potential occurred. A current impulse of 0.01-ms duration was delivered. Maximum MNCVs were calculated based on derived latencies and distance betwee the two stimulating points (16 mm).

At the time of laryngeal fissure creation, recovery of vocal fold movement was also assessed. Recovery was only considered present when equal vocal fold movement on the denervated side was observed compared to the vocal fold on the contralateral nondenervated side. When vocal fold movement on the denervated side was limited (not fixed), recovery was not considered present.

Statistical analysis

Data were analyzed for statistical significance using nonparametric analysis of variance (ANOVA) for comparison among three groups and Mann–Whitney test for comparison between two groups. Values were considered statistically significant at the 5% level.

Acknowledgements

References

1 Isshiki N. Progress in laryngeal framework surgery. Acta Otolaryngol 2000; 120: 120–127.
2 Eisele DW. Complications of thyroid surgery. In: Eisele DW (ed) Complications in Head Neck Surgery. Mosby-Year Book: St Louis, 2000, pp 423–437.
3 Netterville JL, Aly A, Ossoff RH. Evaluation and treatment of complications of thyroid and parathyroid surgery. Otolaryngol Clin North Am 1990; 23: 529–552.
4 Goding GS. Nerve-muscle pedicle reinnervation of the paralyzed vocal cord. Otolaryngol Clin North Am 1991; 24: 1239–1252.

5 Horn KL, Crumley RL. The physiology of nerve injury and repair. *Otolaryngo Clin North Am* 1984; **17**: 321–333.

6 Jacobs IN, Sanders I, Wu BL, Biller HF. Reinnervation of the canine posterior cricoarytenoid muscle with sympathetic preganglionic neurons. *Ann Otol Rhinol Laryngol* 1990; **99**: 167–174.

7 Crumley RL. Mechanisms of synkinesis. *Laryngoscope* 1979; **89**: 1847–1854.

8 Flint PW, Downs DH, Coltrera MD. Laryngeal synkinesis following reinnervation in the rat: neuroanatomic and physiologic study using retrograde fluorescent tracers and electromyography. *Ann Otol Rhinol Laryngol* 1991; **100**: 797–806.

9 Singleton JR, Dixit VM, Feldman EL. Type I insulin-like growth factor receptor activation regulates apoptotic proteins. *J Biol Chem* 1996; **271**: 31791–31794.

10 Kim B, Leventhal PS, Saltiel AR, Feldman EL. Insulin-like growth factor-I-mediated neurite outgrowth *in vitro* requires MAP kinase activation. *J Biol Chem* 1997; **272**: 21268–21273.

11 Russell JW, Windebank AJ, Schenone A, Feldman EL. Insulin like growth factor-I prevents apoptosis in neurons after nerve growth factor withdrawal. *J Neurobiol* 1998; **36**: 455–467.

12 Baumgartner BJ, Shine HD. Targeted transduction of CNS neurons with adenoviral vectors carrying neurotrophic factor genes confers neuroprotection that exceeds the transduced population. *J Neurosci* 1997; **17**: 6504–6511.

13 Ribotta MG, Revah F, Pradier L, Loquet I, Mallet J, Privat A. Prevention of motor neuron death by adenovirus-mediated neurotrophic factors. *J Neurosci Res* 1997; **48**: 281–285.

14 Lewin GR. Neurotrophic factors and pain. *Semin Neurosci* 1995; **7**: 227–232.

15 Dittrich FH, Thoenen H, Sendtner M. Ciliary neurotrophic factor: pharmacokinetics and acute-phase response in rat. *Ann Neurol* 1994; **35**: 151–163.

16 Houenou LJ, Oppenheim RW, Li L, Lo AC, Prevette D. Regulation of spinal motoneuron survival by GDNF during development and following injury. *Cell Tissue Res* 1996; **286**: 219–223.

17 Lapchak PA, Jiao S, Miller PJ, Williams LR, Cummins V, Inouye G *et al.* Pharmacological characterization of GDNF as a therapeutic molecule for treating neurodegenerative diseases. *Cell Tissue Res* 1996; **286**: 179–189.

18 Lindsay RM. Neuron saving schemes. *Nature* 1995; **373**: 289–290.

19 Henderson CE, Phillips HS, Pollock RA, Davies AM, Lemeulle C, Armanini M *et al.* GDNF: a potent survival factor for motoneurons present in peripheral. *Science* 1994; **266**: 1062–1064.

20 Li L, Wu W, Lin LF, Lei M, Oppenheim RW, Houenou LJ. Rescue of adult mouse motoneurons from injury-induced cell death by glial cell line-derived neurotrophic factor. *Proc Natl Acad Sci USA* 1995; **92**: 9771–9775.

21 Yan Q, Matheson C, Lopez OT. In vivo neurotrophic effects of GDNF on neonatal and adult facial motor neurons. *Nature* 1995; **373**: 341–344.

22 Sakamoto T, Watabe K, Ohashi T, Kawazoe Y, Oyanagi K, Inoue K *et al.* Adenoviral vector-mediated GDNF gene transfer prevents death of adult facial motoneurons. *Neuroreport* 2000; **11**: 1857–1860.

23 Nguyen QT, Parsadanian AS, Snider WD, Lichtman JW. Hyperinnervation of neuromuscular junctions caused by GDNF overexpression in muscle. *Science* 1998; **279**: 1725–1729.

24 Hoke A, Cheng C, Zochodne DW. Expression of glial cell line-derived neurotrophic factor family of growth factors in peripheral nerve injury in rats. *Neuroreport* 2000; **11**: 1651–1654.

25 Kang UJ. Genetic modification of cells with retrovirus vectors for grafting into the central nervous system. In: Kaplitt MG, Loewy AD (ed) *Viral Vectors: Gene Therapy and Neuroscience Applications.* Academic Press: San Diego, 1995, pp 211–237.

26 O'Malley Jr BW, Ledley FD. Somatic gene therapy in otolaryngology – head and neck surgery. *Arch Otolaryngol Head Neck Surg* 1993; **119**: 1191–1197.

27 O'Malley Jr BW, Ledley FD. Somatic gene therapy: methods for the present and future. *Arch Otolaryngol Head Neck surg* 1993; **119**: 1100–1177.

28 Shiotani A, O'Malley Jr BW, Coleman ME, Alila HW, Flint PW. Reinnervation of motor endplates and increased muscle fiber size after human insulin-like growth factor I gene transfer into the paralyzed larynx. *Hum Gene Ther* 1998; **9**: 2039–2047.

29 Shiotani A, O'Malley Jr BW, Coleman ME, Flint PW. Human insulin-like growth factor 1 gene transfer into paralyzed rat larynx: single vs multiple injection. *Arch Otolaryngol Head Neck Surg* 1999; **125**: 555–560.

30 Saito K, Shiotani A, Watabe K, Moro K, Fukuda H, Ogawa K. Adenoviral GDNF gene transfer prevents motoneuron loss in the nucleus ambiguus. *Brain Res* 2003; **962**: 61–67.

31 Boulis NM, Bhatia V, Brindle TI, Holman HT, Krauss DJ, Blaivas M *et al.* Adenoviral nerve growth factor and beta-galactosidase transfer to spinal cord: a behavioral and histological analysis. *J Neurosurg* 1998; **90**: 99–108.

32 Liu Y, Himes BT, Moul J, Huang W, Chow SY, Tessler A *et al.* Application of recombinant adenovirus for *in vivo* gene delivery to spinal cord. *Brain Res* 1997; **768**: 19–29.

33 Boulis NM, Turner DE, Dice JA, Bhatia V, Feldman EL. Characterization of adenoviral gene expression in spinal cord after remote vector delivery. *Neurosurgery* 1999; **45**: 131–138.

34 Ghadge GD, Roos RP, Kang UJ, Wollmann R, Fishman PS, Kalynych AM *et al.* CNS gene delivery by retrograde transport of recombinant replication – defective adenoviruses. *Gene Therapy* 1995; **2**: 132–137.

35 Rubin AD, Hogikyan ND, Sullivan K, Boulis N, Feldman EL. Remote delivery of rAAV-GFP to the rat brainstem through the recurrent laryngeal nerve. *Laryngoscope* 2001; **111**: 2041–2045.

36 Rubin A, Mobley B, Hogikyan N, Bell K, Sullivan K, Boulis N *et al.* Delivery of an adenoviral vector to the crushed recurrent laryngeal nerve. *Laryngoscope* 2003; **113**: 985–989.

37 Varejao AS, Cabrita AM, Meek MF, Bulas-Cruz J, Melo-Pinto P, Raimondo S *et al.* Functional and morphological assessment of a standardized rat siatic nerve crush injury with a non-serrated clump. *J Neurotrauma* 2004; **21**: 1652–1670.

38 Bridge P, Ball DJ, Mackinnon SE, Nakao Y, Brandt K, Hunter DA *et al.* Nerve crush injuries – A model for axonotmesis. *Exp Neurol* 1994; **127**: 284–290.

39 Seddon HJ. Three types of nerve injury. *Brain* 1943; **66**: 237.

40 Sunderland S. Classification of peripheral nerve injury producing loss of function. *Brain* 1951; **74**: 491.

41 Zeng L, Worseg A, Albrecht G, Grisold W, Hopf R, Redl H *et al.* A noninvasive functional evaluation following peripheral nerve repair with electromyography in a rat model. *Plast Reconstr Surg* 1994; **94**: 146–151.

42 Carlson SL, Parrish ME, Springer JE, Doty K, Dossett L. Acute inflammatory response in spinal cord following impact injury. *Exp Neurol* 1998; **151**: 77–88.

43 George JA. Gene therapy progress and prospects: adenoviral vectors. *Gene Therapy* 2003; **10**: 1135–1141.

44 Check E. Sanctions agreed over teenager's gene-therapy death. *Nature* 2005; **433**: 674.

45 Raper SE, Chirmule N, Lee FS, Wivel NA, Bagg A, Gao GP *et al.* Fatal systemic inflammatory response syndrome in a ornithine transcarbamylase deficient patient following adenoviral gene transfer. *Mol Genet Metab* 2003; **80**: 148–158.

46 Watabe K, Ohashi T, Sakamoto T, Kawazoe Y, Takeshima T, Oyanagi K *et al.* Rescue of lesioned adult rat spinal motoneurons by adenoviral gene transfer of glial cell line-derived neurotrophic factor. *J Neurosci Res* 2000; **60**: 511–519.

47 Kanegae Y, Takamori K, Sato Y, Lee G, Nakai M, Saito I. Efficient gene activation in mammalian cells by using recombinant adenovirus expressing site-specific Cre recombinase. *Nucl Acid Res* 1995; **23**: 3816–3821.

48 Sakamoto T, Kawazoe Y, Shen JS, Takeda Y, Arakawa Y, Ogawa J *et al.* Adenoviral gene transfer of GDNF, BDNF and TGFβ2, but not CNTF, cardiotrophin-1 or IGF1, protects injured adult motoneurons after facial nerve avulsion. *J Neurosci Res* 2003; **72**: 54–64.

Taylor & Francis
Taylor & Francis Group

ORIGINAL ARTICLE

Association between metallothionein genes polymorphisms and sporadic amyotrophic lateral sclerosis in a Japanese population

YUICHI HAYASHI[1,2], TATSUMA HASHIZUME[1], KENJI WAKIDA[1], MASAHIKO SATOH[3], YOKO UCHIDA[4], KAZUHIKO WATABE[2], ZENJIRO MATSUYAMA[1], AKIO KIMURA[1], TAKASHI INUZUKA[1] & ISAO HOZUMI[1]

[1]*Department of Neurology and Geriatrics, Gifu University Graduate School of Medicine, Gifu,* [2]*Department of Molecular Neuropathology, Tokyo Metropolitan Institute for Neuroscience, Tokyo,* [3]*Department of Hygienics, Gifu Pharmaceutical University, Gifu, and* [4]*Gene Expression Research Group, Tokyo Metropolitan Institute of Gerontology, Tokyo, Japan*

Abstract

Amyotrophic lateral sclerosis (ALS) is a progressive, lethal neurodegenerative disease that selectively affects motor neurons. Reactive oxygen species (ROS) are assumed to be involved in the pathogenesis of ALS. Metallothioneins (MTs) are self-protective, multifunctional proteins that scavenge ROS. In particular, metallothionein-III (MT-III) has a strong scavenging effect on hydroxyl radicals. MTs have been suggested to have important roles in the pathophysiology of ALS. Therefore we investigated single nucleotide polymorphisms (SNPs) of the MT-III and the metallothionein-IIA (MT-IIA) promoter region in 37 Japanese SALS cases and 206 sex-matched healthy controls using polymerase chain reaction (PCR)-direct sequencing or PCR-temporal temperature gradient gel electrophoresis (TTGE). We detected no SNPs of the MT-III gene in SALS cases and controls, and no detectable association between SALS phenotypes and a SNP of the MT-IIA promoter region. We conclude that gene polymorphisms of MT-IIA promoter region and MT-III gene are not associated with SALS phenotypes in a Japanese population.

Key words: *Amyotrophic lateral sclerosis, metallothionein-II, metallothionein-III, single nucleotide polymorphism (SNP)*

Introduction

Amyotrophic lateral sclerosis (ALS) is a lethal neurodegenerative disease with selective loss of motor neurons. Approximately 10% of ALS cases are familial, and 10–25% of these familial ALS (FALS) cases are caused by missense mutations in the Cu/Zn superoxide dismutase (SOD1) gene (1), while others are sporadic ALS (SALS). Reactive oxygen species (ROS) are assumed to play important roles in the pathogenesis of ALS.

Metallothioneins (MTs) are small (6–7 kDa) cystein-rich, metal (Cu/Zn)-binding proteins. MTs are self-protective, multifunctional proteins (2–6) and comprise four members (7,8). Metallothionein-I (MT-I) and metallothionein-II (MT-II) exist ubiquitously and concomitantly in all tissues and are abbreviated as MT-I/-II. MT-IIA is the major isoform of MT-I/-II. Metallothionein-III (MT-III)

and metallothionein-IV are localized mainly in the central nervous system and stratified squamous epithelia, respectively (7,8). MT-III was first named growth inhibitory factor because of inhibition of the survival and neurite formation of cortical neurons (7), and it has a strong scavenging effect on hydroxyl radicals (9).

There have been several reports referring to the associations of MTs with ALS (10–13). The crossing of ALS model mice (G93A SOD1) with MT-I/-II or MT-III knockout mice was found to accelerate the onset or progression of ALS in the progeny, respectively (10). FALS mice reach the onset of clinical signs and death significantly earlier owing to a reduction in MT-I/-II expression level (11). MT-III mRNA is decreased in SALS spinal cords (12). Recently we have shown that the local treatment of an adenoviral vector encoding rat MT-III cDNA prevents the loss of facial motor neurons after facial

nerve avulsion. This paper indicates that MT-III has a therapeutic potential against motor neuron degeneration and injury (6,13).

To clarify the possible protective role of MT in SALS, we investigated the association of polymorphisms of MT genes with susceptibility to SALS, the clinical types, age at onset and progressive rate of SALS in a Japanese population. MT gene polymorphisms are currently available through the databases of the National Center for Biotechnology Information (NCBI, http://www.ncbi.nlm.nih.gov), and Japanese Single Nucleotide Polymorphisms (JSNP, http://snp.ims.u-tokyo.ac.jp). In addition, Kita et al. have recently reported a novel SNP at five bases before the transcription point, SNP (-5) in a Japanese population (14) (Figure 1).

Materials and methods

Samples of SALS cases and controls

Following the acquisition of informed consent, blood was taken from 37 Japanese patients who fulfilled the revised El Escorial criteria (15) for clinically definite and probable ALS (mean age at onset 58.1 ± 11.1 years; 18 females and 19 males; 10 cases were progressive bulbar type, 26 cases classical type and 1 case was pseudopolyneuritic form). Two hundred and six healthy workers and students (95 female, 111 male) of Gifu University and Gifu Pharmaceutical University served as controls. This study was approved by the Ethics Committee of the Gifu University Graduate School of Medicine. Genomic DNA was extracted from peripheral blood samples.

Detection of polymorphisms of the MT-III 3' untranslated region and MT-IIA promoter region

We performed polymerase chain reaction (PCR)-direct sequencing to detect SNPs in the MT-III 3'-untranslated region (UTR) and MT-IIA promoter region. The PCR mixtures contained 1U of Ex Taq polymerase (TaKaRa), 1x Ex Taq PCR buffer (TaKaRa), 200 μM of dNTP mixture (TaKaRa), 80 ng of genomic DNA and 10 pmol each of forward (F) and reverse (R) primers. The PCR cycling conditions consisted of an initial denaturation step at 96°C for 5 min, followed by 30 cycles of 96°C for 1 min, 55°C for 1 min, 72°C for 1 min, and a final extension step at 72°C for 10 min. The forward and reverse primers were given for SNPs in the MT-III 3'-UTR (F: 5'-GAGAGTGGTCATCTTCCATTTTATC-3', R: 5'-CTGTGTGGCTCCCTTGGAATAGGCT-3') and for a SNP in the MT-IIA promoter (F: 5'-CGCCTGGAGCCGCAAGTGAC-3', R: 5'-TGG-GCATCCCCAGCCTCTTA-3'), respectively. The resulting PCR products were purified using a MinElute Gel Extraction Kit (Qiagen). Big Dye Terminator sequencing reactions were performed and sequencing products were analysed on an ABI PRISM 3100 Genetic Analyser (Applied Biosystems).
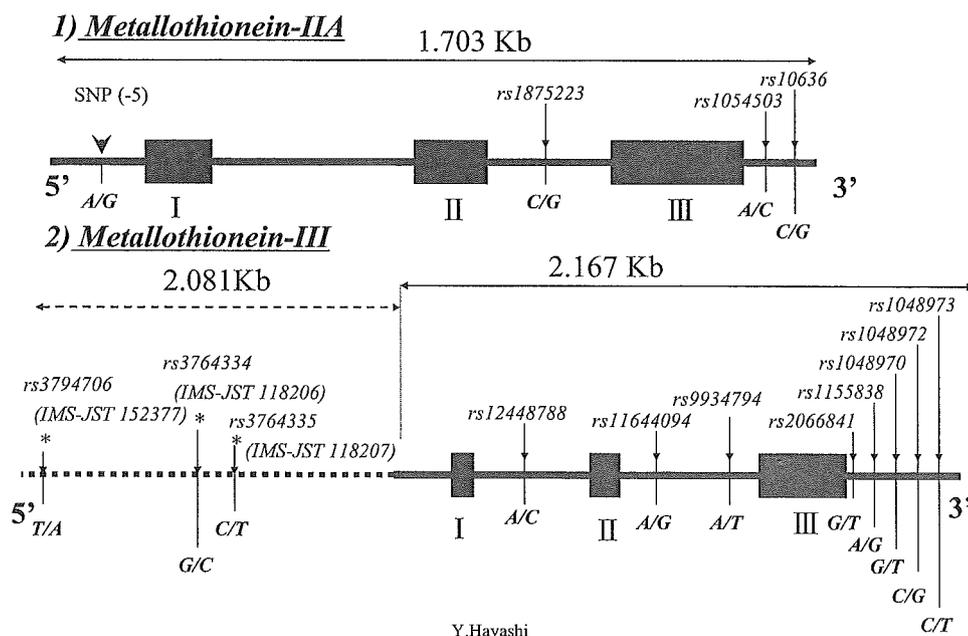

Figure 1. SNPs of metallothionein-IIA and metallothionein-III NCBI database show three SNPs in the MT-IIA gene and eight in the MT-III (arrows), while these 11 SNPs are not found in the JSNP database. The JSNP database shows three SNPs in the 5' up-stream promoter region in MT-III (arrows with asterisk). We performed PCR-direct sequencing or PCR-TTGE for all subjects. We have detected a novel SNP at a 5 bases before the transcription point, SNP (-5) (arrowhead) as recently reported by Kita et al. This SNP has not yet been given SNP ID in both NCBI and JSNP. No SNPs in the MT-III gene could be detected in a Japanese population in our study.

Detection of polymorphisms of MT-III other regions

We performed PCR-temporal temperature gradient gel electrophoresis (TTGE) to detect SNPs in other MT-III regions. The PCR mixtures contained 1U of LA Taq polymerase (TaKaRa), 1x La Taq with GC buffer II (TaKaRa), 200 μM of dNTP mixture (TaKaRa), 200 ng of genomic DNA and 10 pmol each of forward and reverse primers with a GC clump. The PCR cycling conditions were the same as above. We performed TTGE using 7 M urea/6% acrylamide/bis gel and a D-Code Electrophoresis Reagent Kit for TTGE (BIO-RAD). The TTGE conditions were 200 V or 100 V and a gradient temperature from 62°C to 70°C or 65°C to 69°C for 5.3 h or 4 h, respectively. The forward and reverse primers were given for SNPs of the MT-III promoter to exon 1 (F: 5'-GCCCGCCCCCGCCGCCCTGCCCGC GCCCCGCGCCGCCCGCTGGGCTGGCAGT-CGCGGGATAGCG-3', R: 5'-GCGCAGTGC-GCAGGATGCGAGCGGGG-3') and for SNPs of the MT-III introns 1 to 2 (F: 5'-TTCACCG-CCTCCAGCTGCTGCTGT-3', R: 5'-GCG-GGCGGCGCGGGGCGCGGGCAGGCGGCG-GCGGGGGCGGGCGGTCTCCACATCCTGC-GTGGTGAGAC-3'), respectively.

Statistical analyses

Data were statistically analysed using the Welch t-test or χ^2 distribution.

Results

We detected no SNP in the MT-III gene in SALS and controls in our study. In the MT-IIA promoter region, we detected a novel SNP which is the SNP (-5) (Figure 1). The statistical analyses of allele and genotype frequencies showed no significant differences between the SALS and controls (p=0.389 and p=0.293, respectively) (Table I).

Clinically, ALS is divided into three clinical types: classical, progressive bulbar and other forms such as

the pseudopolyneuritic form. In addition, considering the studies using knock-out mice of MT-I/II or MT-III, we divided ALS into two types of progression: the rapid type was the patients within three years before needing a respirator or received percutaneous endoscopic gastrostomy (PEG), and the slow type (more than three years or later).

No association was found between SNP (-5) and SALS phenotypes including clinical type (p=0.488) (Table II), progression rate (p=0.905) (Table III) and age at onset (p=0.297) (Table IV). We compared SNP (-5) with age at onset for each clinical or progression type of SALS. No association was found between SNP (-5) and age at onset in the classical type (p=0.681), bulbar type (p=0.084), or slow type (p=0.797) (Table IV). With regard to the rapid type, we were unable to obtain adequate numbers of large samples sufficient for the t-test.

Discussion

MT is one of the candidate genes associated with the pathophysiological mechanism of SALS (12). Recently Morahan et al. have reported that MT-III gene polymorphisms are unlikely to be responsible for susceptibility to SALS in an Australian population (16). We investigated polymorphisms of MT-III and MT-IIA promoter region in SALS cases and healthy controls in a Japanese population. We detected no SNP in the MT-III gene and detected a novel SNP in the MT-IIA promoter region as reported by Kita et al. (14). The NCBI

Table II. Clinical types and genotypes in SNP (-5) in the MT-IIA.

Clinical type	Number	A/A	A/G	G/G	p value
Bulbar type	10	7	3	0	0.488
Classical type	26	21	5	0	

Statistical analysis was performed by χ^2 distribution.

Table I. Association analysis of SNP (-5) in the MT-IIA.

Samples	Number	A/A	A/G	G/G	p value (genotype)	MAF	p value (allele)
Total							
SALS	37	28	9	0	0.293	0.122	0.389
Controls	206	170	35	1		0.090	
Female							
SALS	18	13	5	0	0.582	0.139	0.487
Controls	95	77	17	1		0.100	
Male							
SALS	19	15	4	0	0.603	0.105	0.621
Controls	111	93	18	0		0.081	

MAF: Minor allele frequency; SALS: sporadic amyotrophic lateral sclerosis. Statistical analysis was performed by χ^2 distribution.

Table III. Progression and genotypes in SNP (-5) in the MT-IIA.

Progression	Number	A/A	A/G	G/G	p value
Rapid type	5	4	1	0	0.905
Slow type	17	14	3	0	

Statistical analysis was performed by χ^2 distribution.

Table IV. Age at onset and genotypes in SNP (-5) in the MT-IIA.

Clinical type	A/A	A/G	p value
SALS total $(n=37)$ (y)	59.34 ± 12.34	55.89 ± 6.77	0.297
Bulbar type $(n=10)$ (y)	71.00 ± 10.40	59.00 ± 7.21	0.084
Classical type $(n=26)$ (y)	55.86 ± 10.71	56.40 ± 4.77	0.681
Slow type $(n=17)$ (y)	53.43 ± 10.49	52.00 ± 7.55	0.797
Rapid type* $(n=5)$ (y)	68.50 ± 9.95	56.00**	**

Age at onset (mean age $\pm$ SD (years)), n: number. y: years *,**: In the rapid type, we were unable to obtain large samples sufficiently for the t-test. Statistical analysis was performed by Welch t-test.

SNP database shows that human MT-III gene has eight SNPs and MT-IIA has three SNPs (Figure 1), while these SNPs are not found in the JSNP database. The difference between the SNP databases is assumed to be due to the difference in races. In our study we were unable to identify a significant association between SNP in the MT-IIA promoter region, and SALS phenotypes including susceptibility to SALS, clinical types, age at onset and progressive rate of SALS. These results will be required to replicate in large sample sets from various ethnic groups.

Conclusion

No clear association was found between SNP in the MT-IIA promoter region and SALS phenotypes, and we detected no SNP in all MT-III gene in Japanese SALS and controls.

Appendix

The JSNP database has very recently shown three SNPs in the 5' far up-stream promoter region in MT-III in Japanese population on web site.

Acknowledgements

References

1. Cudkowicz ME, McKenna-Yasek D, Sapp PE, Chin W, Geller B, Hayden DL, et al. Epidemiology of mutations in superoxide dismutase in amyotrophic lateral sclerosis. Ann Neurol. 1997;41:210–21.
2. Vallee BL. The function of metallothionein. Neurochem Int. 1995;27:23–33.
3. Miles AT, Hawksworth GM, Beattie JH, Rodilla V. Induction, regulation, degradation, and biological significance of mammalian metallothioneins. Crit Rev Biochem Mol Biol. 2000;35:35–70.
4. Montoliu C, Monfort P, Carrasco J, Palacios O, Capdevila M, Hidalgo J, et al. Metallothionein-III prevents glutamate and nitric oxide neurotoxicity in primary cultures of cerebellar neurons. J Neurochem. 2000;75:266–73.
5. Ren H, Ji Q, Liu Y, Ru B. Different protective roles in vitro of α- and β-domains of growth inhibitory factor (GIF) on neuron injuries caused by oxygen free radicals. Biochim Biophys Acta. 2001;568:129–34.
6. Hozumi I, Asanuma M, Yamada M, Uchida Y. Metallothioneins and neurodegenerative diseases. J Health Science. 2004;50:323–31.
7. Uchida Y, Takio K, Titani K, Ihara Y, Tomonaga M. The growth inhibitory factor which is deficient in the Alzheimer's disease brain is a 68 amino acid metallothionein-like protein. Neuron. 1991;7:337–47.
8. Quaife CJ, Findley SD, Froelick JG, Kelly EJ, Zambrowics BP, Palmiter RD. Induction of a new metallothionein isoform (MT-IV) occurs during differentiation of stratified squamous epithelia. Biochemistry. 1994;33:7250–9.
9. Uchida Y, Gomi F, Masumizu T, Miura Y. Growth inhibitory factor prevents neurite extension and the death of cortical neurons caused by high oxygen exposure through

hydroxyl radical scavenging. J Biol Chem. 2002;277: 32353–9.

10. Nagano S, Satoh M, Sumi H, Fujimura H, Tohyama C, Yanagihara T, et al. Reduction of metallothioneins promotes the disease expression of familial amyotrophic lateral sclerosis mice in a dose-dependent manner. Eur J Neurosci. 2001;13:1363–70.

11. Puttaparthi K, Gitomer WL, Krishnan U, Son M, Rajendran B, Elliott JL. Disease progression in a transgenic model of familial amyotrophic lateral sclerosis is dependent on both neuronal and non-neuronal zinc binding proteins. J Neurosci. 2002;22:8790–6.

12. Ishigaki S, Niwa J, Ando Y, Yoshihara T, Sawada K, Doyu M, et al. Differentially expressed genes in sporadic amyotrophic lateral sclerosis spinal cords screening by molecular indexing and subsequent cDNA microarray analysis. FEBS lett. 2002;531:354–8.

13. Sakamoto T, Kawazoe Y, Uchida Y, Hozumi I, Inuzuka T, Watabe K. Growth inhibitory factor prevents degeneration of injured adult rat motor neurons. NeuroReport. 2003;14: 2147–51.

14. Kita K, Miura N, Naganuma A. Effect of polymorphism in the promoter of the human gene for metallothionein IIA on its transcription. Seikagaku Abstr. 2002;74:964. (In Japanese.)

15. Brooks BR, Miller RG, Swash M, Musat TL. World Federation of Neurology Research Group on Motor Neuron Diseases. El Escorial revisited: revised criteria for the diagnosis of amyotrophic lateral sclerosis. Amyotroph Lateral Scler Other Motor Neuron Disord. 2000;1:293–9.

16. Morahan JM, Yu B, Trent RJ, Pamphlett R. Screening the metallothionein III gene in sporadic amyotrophic lateral sclerosis. Amyotroph Lateral Scler Other Motor Neuron Disord. 2005;6:115–7.

ORIGINAL ARTICLE

Mai Ohsawa · Masaharu Kotani · Youichi Tajima
Daisuke Tsuji · Yasuhiro Ishibashi · Aya Kuroki
Kohji Itoh · Kazuhiko Watabe · Kazunori Sango
Shoji Yamanaka · Hitoshi Sakuraba

Establishment of immortalized Schwann cells from Sandhoff mice and corrective effect of recombinant human β-hexosaminidase A on the accumulated GM2 ganglioside

Abstract We have established spontaneously immortalized Schwann cell lines from dorsal root ganglia and peripheral nerves of Sandhoff mice. One of the cell lines exhibited genetically and biochemically distinct features of Sandhoff Schwann cells. The enzyme activities toward 4-methylumbelliferyl *N*-acetyl-β-D-glucosamine (β-hexosaminidases A, B, and S) and 4-methylumbelliferyl *N*-acetyl-β-D-glucosamine-6-sulfate (β-hexosaminidases A and S) were decreased, and GM2 ganglioside accumulated in lysosomes of the cells. Incorporation of recombinant human β-hexosaminidase isozymes expressed in Chinese hamster ovary cells into the cultured Sandhoff Schwann cells via cation-independent mannose 6-phosphate receptors was found, and the incorporated β-hexosaminidase A degraded the accumulated GM2 ganglioside. The established Sandhoff Schwann cell line is useful for investigation and development of therapies for Sandhoff disease.

Keywords Sandhoff disease · β-Hexosaminidase · GM2 ganglioside · Schwann cell · Lysosomal disease · Enzyme replacement therapy

M. Ohsawa · M. Kotani · Y. Tajima · D. Tsuji · Y. Ishibashi
A. Kuroki · K. Itoh · K. Watabe · H. Sakuraba
CREST, JST, Kawaguchi, Japan

M. Ohsawa · M. Kotani · Y. Tajima · H. Sakuraba (✉)
Department of Clinical Genetics,
The Tokyo Metropolitan Institute of Medical Science,
Tokyo Metropolitan Organization for Medical Research,
3-18-22 Honkomagome, Bunkyo-ku, Tokyo 113-8613, Japan
E-mail: sakuraba@rinshoken.or.jp
Tel.: +81-3-38232105
Fax: +81-3-38236008

D. Tsuji · Y. Ishibashi · A. Kuroki · K. Itoh
Department of Medicinal Biotechnology,
Institute for Medicinal Resources,
Graduate School of Pharmaceutical Sciences,
The University of Tokushima, Tokushima, Japan

K. Watabe
Department of Molecular Neuropathology,
Tokyo Metropolitan Institute for Neuroscience,
Tokyo Metropolitan Organization for Medical Research,
Tokyo, Japan

K. Sango
Department of Developmental Morphology,
Tokyo Metropolitan Institute for Neuroscience,
Tokyo Metropolitan Organization for Medical Research,
Tokyo, Japan

S. Yamanaka
Department of Pathology, School of Medicine,
Yokohama City University, Yokohama, Japan

Introduction

β-Hexosaminidase (Hex; EC 3. 2. 1. 52) is a lysosomal glycosyl hydrolase that catalyzes the hydrolysis of β-1,4-linked *N*-acetyl hexosamine residues at the nonreducing ends of glycoconjugates. The human *HEXA* and *HEXB* genes code for the α-subunit and β-subunit of Hex, which dimerize to produce two major isozymes—β-hexosaminidase A (Hex A, αβ heterodimer) and β-hexosaminidase B (Hex B, ββ homodimer)—and a minor, unstable isozyme, β-hexosaminidase S (Hex S, αα homodimer). All of the Hex isozymes basically degrade terminal *N*-acetylgalactosamine (GalNAc) and *N*-acetylglucosamine (GlcNAc) residues while Hex A and Hex S cleave off terminal *N*-acetylglucosamine-6-sulfate residues, and only Hex A among the three isozymes can degrade GM2 ganglioside by acting on a complex of GM2 ganglioside and the GM2 activator encoded by *GM2A* (Gravel et al. 2001). The 4-methylumbelliferyl *N*-acetyl-β-D-glucosamine (MUG) and 4-methylumbelliferyl *N*-acetyl-β-D-glucosamine-6-sulfate (MUGS) are usually used as artificial substrates for enzyme assaying of the total Hex isozymes and for that of Hex A and Hex S, respectively. The defect of the *HEXB* gene causes

Sandhoff disease with simultaneous deficiencies of both Hex A and Hex B, which result in storage of GM2 ganglioside in the nervous system and accumulation of oligosaccharides and glycoproteins with GlcNAc residues at the nonreducing ends of the sugar chains in the extraneuronal tissues. Sandhoff disease involves progressive neurological disorders and exhibits a wide clinical spectrum from the severe infantile form (classical Sandhoff disease), which is of early onset and fatal before the age of 4 years, to the late onset and less severe form, which allows survival into childhood or adulthood (subacute and chronic forms and atypical Sandhoff disease). Patients with the severe infantile form of Sandhoff disease develop progressive psychomotor delay, muscular weakness, hypotonia, visual disturbance, cherry-red spots, seizures, macrocephaly, and hepatosplenomegaly. Patients with the milder, late-onset form of Sandhoff disease develop dystonia, ataxia, incoordination, muscle wasting, and weakness. However, the common pathological and biochemical changes in the various clinical forms of Sandhoff disease are ultrastructurally identified membranous cytoplasmic inclusion bodies and accumulation of GM2 ganglioside, respectively, in the central and peripheral nervous systems (Gravel et al. 2001).

Recently, a mouse model of Sandhoff disease was created through the targeted disruption of the *Hexb* gene, which encodes mouse Hex β-subunit (Sango et al. 1995; Phaneuf et al. 1996). Sandhoff mice exhibit progressive neurological disorders consistent with the corresponding human disease, and morphological changes specific for this disease are found in neurons of the cerebrum, cerebellum, spinal cord, dorsal root ganglia (DRG) and visceral organs, satellite cells, and Schwann cells (Sango et al. 1995, 2002), suggesting storage of GM2 ganglioside in these neuronal cells.

Enzyme replacement therapy (ERT) has been introduced for lysosomal diseases, including Gaucher disease (Barton et al. 1991), Fabry disease (Schiffmann et al. 2000; Eng et al. 2001), and mucopolysaccharidosis (MPS) I (Wraith et al. 2004); clinical trials for Pompe disease (Van den Hout et al. 2004; Klinge et al. 2005), MPS II (Muenzer et al. 2002), and MPS VI (Harmatz et al. 2004) are underway. Furthermore, therapeutic experiments have also been performed for other lysosomal diseases associated with neurological disorders, including Sandhoff disease (Dobrenis et al. 1992). In these experiments, cell lines possessing distinct phenotypes of the nervous system are required to detect cleavage of the accumulated substances from the neuronal cells after treatment. However, such kinds of cell lines had not been established yet for Sandhoff disease. They would be useful for clarification of the pathogenesis of Sandhoff disease and the development of therapies for the disease.

In this study, we established spontaneously immortalized Schwann cell lines from DRG and peripheral nerves of Sandhoff mice and examined their uptake of the recombinant Hex isozymes produced by Chinese hamster ovary (CHO) cell lines simultaneously expressing the human *HEXA* and *HEXB* genes and degradation of the accumulated GM2 ganglioside. The effects of the recombinant Hex isozymes on the cultured Sandhoff Schwann cells were compared with those on cultured fibroblasts from a patient with Sandhoff disease.

Materials and methods

Animals and cell culture

C57BL/6 Sandhoff mice homozygous for the disrupted *Hexb* gene (Sango et al. 1995) were used in this experiment according to the rules drawn up by the Animal Care Committee of our institute. Primary and long-term cultures of DRG and adjacent peripheral nerves collected from 8-week-old Sandhoff mice were performed and spontaneously immortalized Schwann cells were obtained, as previously described (Watabe et al. 1990, 1994, 1995, 2001). Among them, an established Schwann cell line from a Sandhoff mouse (1113C1) was cultured in Iscove's modified Dulbecco's minimum essential medium supplemented with 5% fetal calf serum (FCS), 50 units/ml penicillin, and 50 μg/ml streptomycin at 37°C under a 5% CO_2–95% air mixture. Spontaneously immortalized Schwann cells were obtained from CD-1 (ICR) wild-type mice, and an established cell line (IMS32) was used as a control (Watabe et al. 1995).

Cultured skin fibroblasts from a patient with Sandhoff disease and a normal subject were established and maintained in our laboratory. The study involving the cultured fibroblasts was approved by the Ethical Committee of our institution. The cells were cultured in Ham's F-10 medium supplemented with 10% FCS and antibiotics at 37°C in a humidified incubator flushed continuously with a 5% CO_2–95% air mixture.

Polymerase chain reaction

Confirmation of the genotype of the established cultured Schwann cells was performed by means of polymerase chain reaction (PCR), as previously described (Sango et al. 2002). Reverse transcription followed by PCR (RT-PCR) was performed to identify Schwann-cell-associated molecules, i.e., S100, p75^{NTR}, L1, peripheral myelin protein zero (P0), peripheral myelin protein-22 (PMP-22), and growth-associated protein-43 (GAP-43), as described elsewhere (Mirsky and Jessen 1999; Watabe et al. 2001, 2003).

Immunocytochemical analysis of Schwann-cell-associated markers

To characterize the established cultured Schwann cells, immunocytochemical analysis of S100, laminin, and glial fibrillary acidic protein (GFAP) was performed, as described previously (Watabe et al. 1995, 2003).

462

Enzyme assays and protein determination

Total Hex (Hex A, Hex B, and Hex S) activity in cultured cells was determined with MUG (Nacalai Tesque, Kyoto, Japan) as a substrate (Suzuki 1987). Enzyme activity for Hex A and Hex S was determined with MUGS (HSC Research Development Co., Toronto, Canada) as a substrate, according to the manufacturer's method. Protein determination was performed with a Bio-Rad dye-binding assay kit (Bio-Rad, Hercules, CA, USA) using bovine serum albumin as a standard.

Preparation of the recombinant human Hex isozymes produced in CHO cells

A CHO cell line simultaneously expressing the human Hex α-subunit and β-subunit were established by means of cointroduction of the human *HEXA* and *HEXB* cDNAs, as described elsewhere (Sakuraba et al. 2005). The CHO cells stably expressing Hex isozymes, including Hex A, Hex B, and Hex S, were cultured in serum-free Ham's F-10 medium. After 3 days of incubation, the culture medium was harvested and used as the conditioned medium.

Administration of the Hex isozymes to cultured mouse Sandhoff Schwann cells and cultured human Sandhoff fibroblasts

To examine the uptake of the Hex isozymes and cleavage of the accumulated GM2 ganglioside by the incorporated Hex A, cultured mouse Sandhoff Schwann cells and cultured human Sandhoff fibroblasts were cultured on 6-well plates in the conditioned medium containing Hex isozymes in the presence or absence of 5 mM mannose 6-phosphate (M6P). Because Hex A is heat-labile, a half volume of the culture medium was replaced daily by the same volume of fresh medium containing the same levels of MUG-degrading and MUGS-degrading activities, and then the cultured cells were harvested for enzyme assays or fixed with 4.5% paraformaldehyde for an immunocytochemical analysis of intracellular GM2 ganglioside, as described below.

Immunocytochemical analysis of intracellular GM2 ganglioside

To examine the accumulation and localization of GM2 ganglioside in the cultured cells, double immunostaining with a monoclonal anti-GM2 ganglioside antibody (IgM isotype; Kotani et al. 1992) and affinity-purified goat polyclonal antibodies against lysosome-associated membrane protein-1 (LAMP-1) (IgG isotype; Santa Cruz Biochemistry, Santa Cruz, CA, USA) was performed, as described previously (Sakuraba et al. 2002).

The stained cells were examined under a microscope (Axiovert 100M; Carl Zeiss, Oberkochen, Germany) equipped with a confocal laser scanning imaging system (LSM510; Carl Zeiss).

Results

Characterization of the established Schwann cells derived from a Sandhoff mouse

The Schwann cell lines established from Sandhoff mice were spindle-shaped and not contact-inhibited. One of the cell lines, designated as 1113Cl, was used in this study. To determine the genotype of the established Schwann cells, a genomic DNA fragment of 114-bp in the *Hexb* wild-type locus and a 219-bp DNA fragment in the targeted locus were amplified by means of PCR, according to the method described previously (Sango et al. 1995). As shown in Fig. 1, a 219-bp DNA fragment in the targeted locus was detected for 1113Cl while a 114-bp band in the wild-type locus was observed for IMS32. The results confirmed that 1113Cl is genetically homozygous for the disrupted *Hexb* gene.
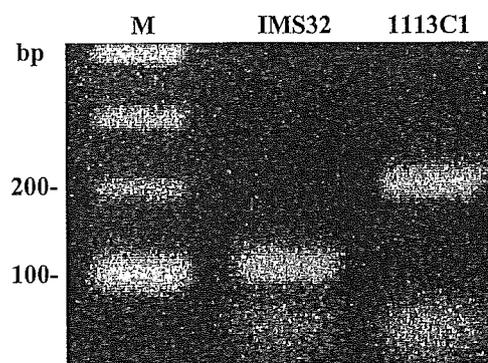

Fig. 1 Genomic PCR analysis of *Hexb* in IMS32 and 1113Cl cells. PCR amplification from IMS32 cells results in a 114-bp fragment and that from 1113Cl cells in a 219-bp fragment
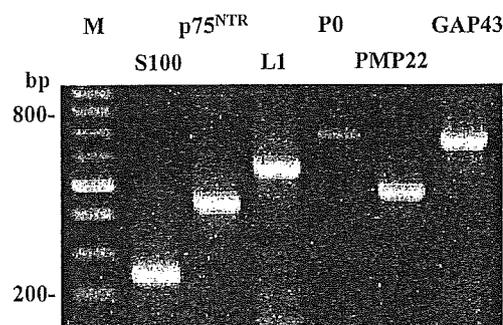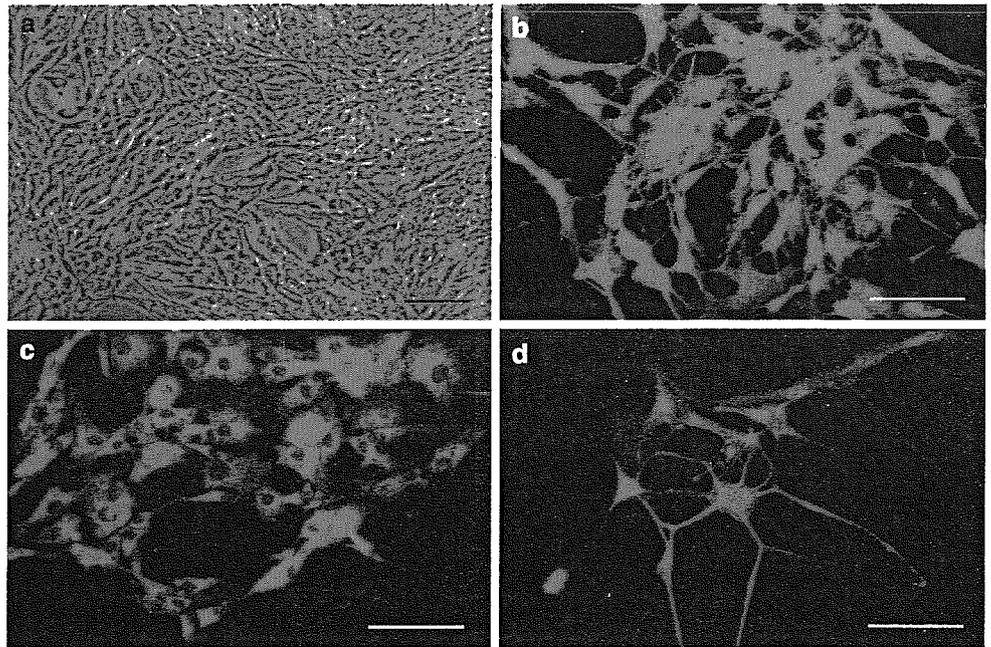

Fig. 2 RT-PCR analysis of 1113Cl cells. The 100-bp DNA size markers (*M*) and amplified PCR fragments of S100, p75[NTR], L1, P0, PMP22, and GAP43

Fig. 3 Phase-contrast and immunofluorescence microscopy of 1113C1 cells. Phase-contrast microscopy of living cells (**a**), and immunofluorescence for S100 (**b**), laminin (**c**), and GFAP (**d**). *Bars*, 50 μm

RT-PCR demonstrated mRNA expression of S100, $p75^{NTR}$, L1, P0, PMP22, and GAP43 (Fig. 2), and immunocytochemical analysis also revealed protein expression of S100, laminin, and GFAP in 1113C1 (Fig. 3). These results indicate the distinct Schwann cell phenotype of 1113C1.

To investigate the localization and accumulation of GM2 ganglioside in the cultured Sandhoff Schwann cells, double staining was performed with a monoclonal antibody for GM2 ganglioside and polyclonal antibodies for LAMP-1 as a lysosomal marker. Intense granular immunofluorescence for GM2 ganglioside was observed in 1113C1 while only faint fluorescence was found in IMS32, and the localization was coincident with that of LAMP-1 (Fig. 4a). Enhanced immunofluorescence for LAMP-1 was also observed in 1113C1. These results suggested increased and enlarged lysosomes containing abundant gangliosides in Schwann cells derived from a Sandhoff mouse. The intensity of the immunofluorescence for GM2 ganglioside in 1113C1 was almost the same as that in cultured human Sandhoff fibroblasts (Fig. 4b). The MUGS-degrading and MUG-degrading activities in 1113C1 were 19% and 5% of the control values, respectively (Table 1). The MUGS-degrading and MUG-degrading activities are slightly higher than those for cultured human Sandhoff fibroblasts (Table 1).

Enzyme replacement effect of recombinant human Hex isozymes on the intracellular Hex activities and cleavage of GM2 ganglioside in cultured mouse Sandhoff Schwann cells

We investigated the uptake of the recombinant human Hex isozymes by mouse Sandhoff Schwann cells in culture and compared it with that in the case of cultured human Sandhoff fibroblasts. The conditioned medium from the CHO transformants expressing the human α-subunit and β-subunit cDNAs was administered to mouse Sandhoff Schwann cells and human Sandhoff fibroblasts. The MUGS-degrading and MUG-degrading activities in the conditioned medium were 299 and 758 nmol/h per milliliter, respectively. As shown in Table 1, the intracellular MUGS-degrading and MUG-degrading activities in the mouse Sandhoff Schwann cells were increased by 30% and 33% compared with the normal control values after 3 days of culture in the conditioned medium while those in the human Sandhoff fibroblasts were restored by 66% and 99%, respectively. The uptake of the recombinant Hex isozymes was inhibited in the presence of 5 mM M6P in the culture medium.

We also investigated the effect of incorporated Hex A on the degradation of GM2 ganglioside accumulated in the mouse Sandhoff Schwann cells (Fig. 5a) and human Sandhoff fibroblasts (Fig. 5b). The GM2 ganglioside accumulated in the mouse Sandhoff Schwann cells was cleaved on 3 days of culture with the conditioned medium containing Hex A as well as in the human Sandhoff fibroblasts. The enhanced immunofluorescence for LAMP-1 was also normalized by this procedure. The effect was inhibited by the addition of M6P to the culture medium.

Discussion

In this study, we established a spontaneously immortalized Schwann cell line, 1113C1, from DRG and peripheral nerves of Sandhoff mice. The 1113C1 cells possess the disrupted *Hexb* gene allele and exhibit a
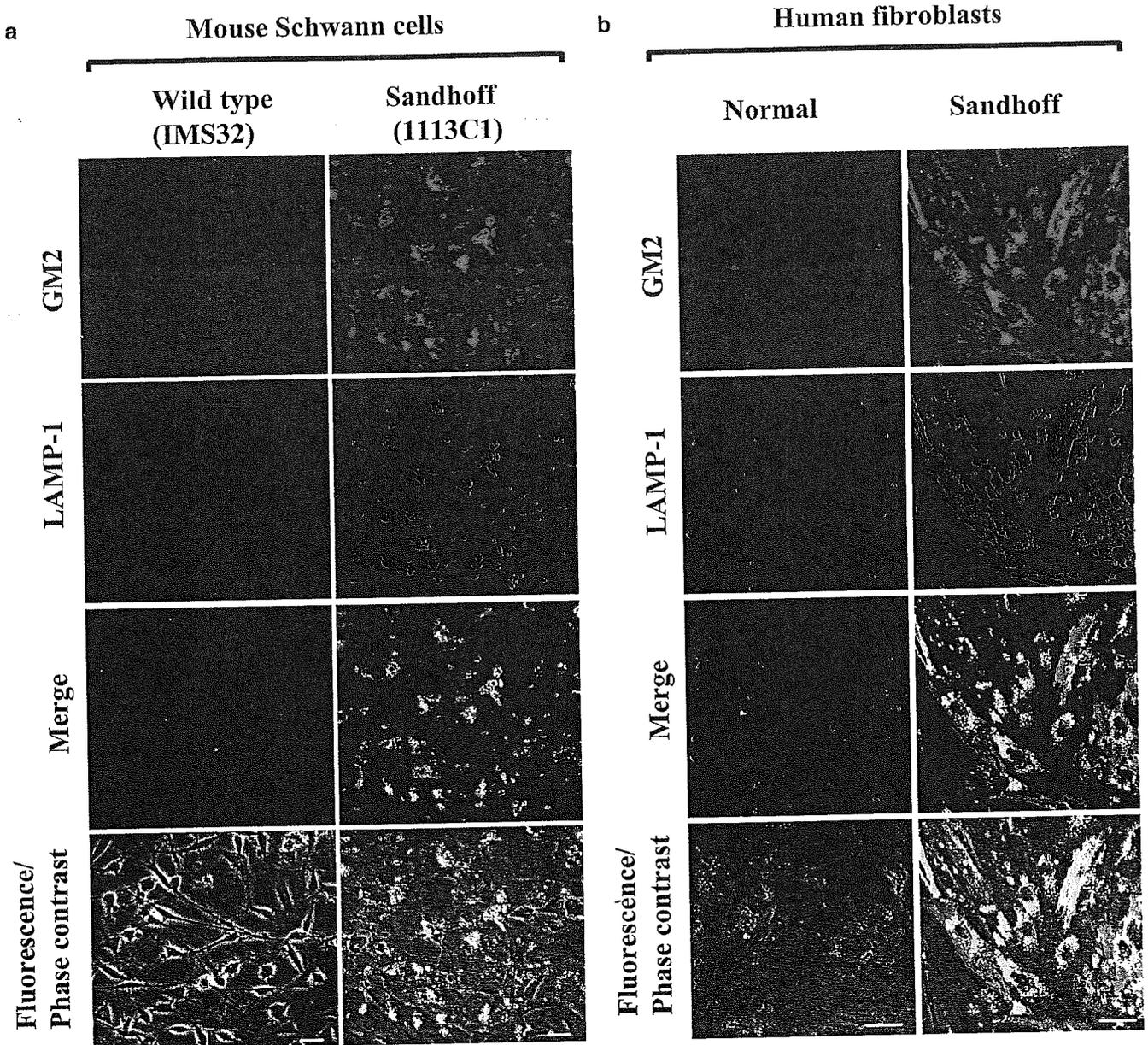
a Mouse Schwann cells

Wild type (IMS32) | Sandhoff (1113C1)

GM2 / LAMP-1 / Merge / Fluorescence/Phase contrast

b Human fibroblasts

Normal | Sandhoff

GM2 / LAMP-1 / Merge / Fluorescence/Phase contrast

Fig. 4 Immunocytochemical analysis of intracellular GM2 ganglioside. Double staining of cultured mouse Schwann cells (a) and human fibroblasts (b) was carried out using a monoclonal antibody for GM2 ganglioside (*GM2, green*) and polyclonal antibodies for LAMP-1 (*LAMP-1, red*). Overlapped images with these two fluorescent probes are shown in *yellow* (*Merge*). *Fluorescence/Phase contrast* shows overlapped Merge and phase-contrast images. *Bars*, 50 μm

distinct Schwann cell morphology and biochemical phenotypes such as S100, p75[NTR], L1, P0, PMP-22, GAP-43, laminin, and GFAP, as shown on RT-PCR and/or immunocytochemical analysis. Moreover, immunocytochemical analysis revealed the accumulation of GM2 ganglioside in lysosomes of 1113C1 cells as well as in those of cultured human Sandhoff fibroblasts. The reason the 1113C1 cells have residual MUGS-degrading and MUG-degrading activities has not been clarified yet. However, as the disruption of the mouse Hex β-subunit gene and the accumulation of GM2 ganglioside due to decreased Hex A activity are characterized in this cell line, the residual activity must be mainly resulted from

Hex S (αα homodimer). Culture condition and/or tissue specificity might influence the formation of αα homodimer. Considering the analytical data, the 1113C1 cell lines are thought to be useful for clarifying the pathophysiology of Sandhoff disease and for examining effects in the therapeutic experiments on this disease.

We obtained the recombinant Hex isozymes from the CHO cell line coexpressing the human Hex α-subunit and β-subunit cDNAs. The MUGS-degrading and MUG-degrading activities increased in 1113C1 cells on culturing them in conditioned medium containing the expressed Hex isozymes although the degrees of the increases of the enzyme activities were lower than that in the cultured